New Solid State Laser System for SPES:Selective Production of Exotic Species project at Laboratori Nazionali di Legnaro

D.Scarpa,[1, a)] E.Mariotti,[2] O.S. Khwairakpam,[2,1] V. Parenti,[2] A. Buono,[2] P. Nicolosi,[3] M.Calderolla,[4] A. Khanbekyan,[5] M. Ballan,[1] L. Centofante,[6] S. Corradetti,[1] G. Lilli,[1] M. Manzolaro,[1] A. Monetti,[1] L. Morselli,[1] and A. Andrighetto[1]

[1)] *Istituto Nazionale de Fisica Nucleare - Laboratori Nazionali di Legnaro - Viale Università 2, 35020 Legnaro (PD)- Italy*

[2)] *Università di Siena 1240 - Dipartimento di Scienze Fisiche, della Terra e dell'Ambiente, sezione di Fisica - via Roma 56, 53100 Siena - Italy, INFN sezione di Pisa*

[3)] *Università degli Studi di Padova - LUXOR CNR IFN - Via Trasea 7, 35131 Padova - Italy*

[4)] *Azienda ULSS n.1 - Viale Europa 22, 32100 Belluno - Italy*

[5)] *Università degli Studi di Ferrara -Dipartimento di Fisica e Scienze della Terra - Via Giuseppe Saragat 1, 44122 Ferrara - Italy*

[6)] *Università degli Studi di Brescia - Dipartimento di Ingegneria Meccanica ed Industriale - via Branze 38, 25125, Brescia, Italy - Italy*

(Dated: 18 May 2022)

The SPES:Selective Production of Exotic Species project is under construction at Laboratori Nazionali di Legnaro (LNL)-INFN. The aim of the collaboration is to produce highly pure RIBs:Radioactive Ion Beams from fission fragments of a uranium carbide (UC_x) target activated by a cyclotron proton beam. In order to select a specific atomic species, the main tool to be applied is the resonant laser ionization technique. We have just completed the installation of a dedicated all solid state laser system whose elements are tunable to transitions of all of the elements/isotopes of interest for the project. The new laser system is based on three TiSa:Titanium Sapphire laser sources, independently pumped by three Nd:YLF pump lasers and it can be coupled to two high harmonic generation (SHG:Second Harmonic Generation, THG:Third Harmonic Generation, FHG:Fourth Harmonic Generation) setups. Power, wavelength and position of the laser beams are continuously monitored and stabilized by automated active systems to improve RIB beam production stability. The paper presents the main features of the laser system and examples of application of a LIS:Laser Ion Source , including a first demonstration of photoionization of stable silver, one of the most requested elements for RIB application.

I. SELECTIVE PRODUCTION OF EXOTIC SPECIES AT LABORATORI NAZIONALI DI LEGNARO

A. SPES Project.

During the last thirty years, the realization of radioactive beam facilities has represented one of the most important technical advances for nuclear physics research[1], as well as for interdisciplinary science and, in particular, for the special applications of radiopharmacology[2].

The development of new big infrastructures has been realized both by a reconversion and refurbishment of already existing machines and by the design and construction of dedicated facilities. In fact, RIBs have already provided research opportunities otherwise not available with stable elements. As a few examples, RIBs allow for 1) a better understanding of the properties of nuclei, going back to the period of their formation in the early universe[3]; 2) the investigation of nuclear reactions, far from the stability region, fundamental to the stellar nucleosynthesis[4]; 3) the determination of the behavior of many-body systems[5]. At Legnaro INFN Laboratory, the project SPES, which is the acronym for "Selective Production of Exotic Species", is devoted to the development and installment of a second generation ISOL:Isotope Separation On-Line facility[6,7]. Currently, it is in the final period of the construction phase. The infrastructure will accelerate, when a uranium carbide target is used, radioactive neutron-rich nuclei in the range of mass 80-160 amu with an estimated fission rate of about $10^{13}s^{-1}$ (incident proton beam: I=200 A, E=40 MeV). Neutron-deficient beams will be obtained using other target materials, such as silicon carbide, currently under development. The produced beams will be used for studies in fundamental nuclear physics, as well as for applications, ranging from the production of radionuclides of medical interest to the generation of neutrons for material studies, nuclear technologies and medicine. A general overview of the SPES ISOL facility is reported in Fig.1; a detailed view of the laser laboratory position and of the laser beam path to the ion source is shown in Fig.2. A primary proton beam of energy ranging from 35 to 70 MeV (up to 70 kW of power) is extracted from the driver cyclotron (A) and sent to the RIB production bunker, where in the front-end apparatus, nuclear reactions occur in the installed production target (B). The Front End includes all the devices necessary for the ionization and the first acceleration of the beam, while a first mass separation of the

[a)]The author to whom correspondence may be addressed: daniele.scarpa@lnl.infn.it

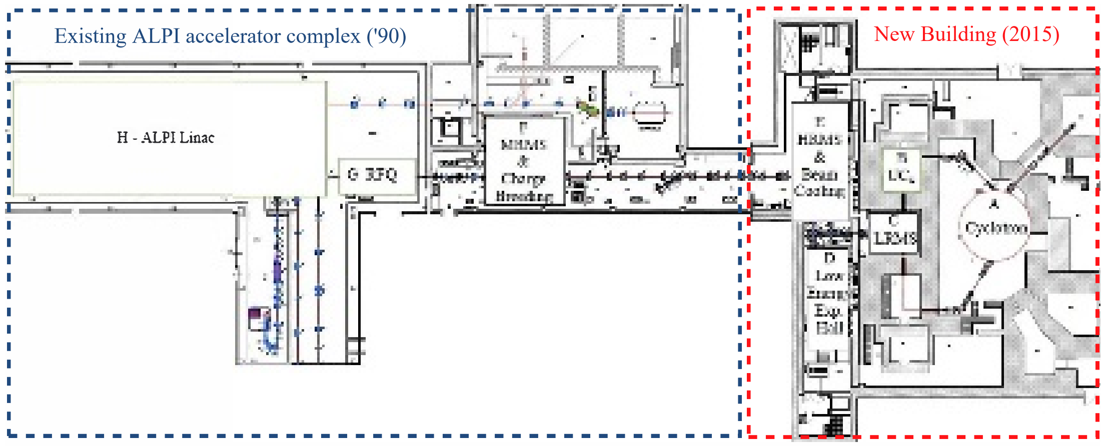

FIG. 1. Layout of the SPES facility: A-Cyclotron, B-UC$_x$Production Target bunker, C-Low Resolution Mass Separator (LRMS), D-Experimental Hall for low energy (up to 40 keV) experiments, E-Beam cooling and High Resolution Mass Separator (HRMS), F-Charge breeding and Medium Resolution Mass Separator (MRMS), G-RFQ, H-ALPI linac.

produced isotopes is performed by a Wien Filter. The obtained low energy (up to 40 keV) isobaric beam, going through various electrostatic devices including electrostatic quadrupole triplets, electrostatic dipoles and steerers and after being bent by the 90° magnet analyzer (C - LRMS:Low Resolution Mass Separator), is injected into a Beam Cooler, an apparatus capable of decreasing the transverse and longitudinal beam emittance. The LRMS is also used as the entry point for the laser beam coming from the Online Laser Laboratory placed at the first floor of the building, directly on top of the LRMS hall as shown in Fig. 2. Finally, the second step of beam purification is performed in a HRMS:High-Resolution Mass Separator (E). The obtained isotopically pure RIB can be either directly provided to users for low energy experiments (D) or, eventually, be injected into a Charge Breeder, a device devoted to increase the beam charge state, and MRMS:Medium Resolution Mass Separator (F). The post-acceleration will be performed by coupling the RFQ:Radio Frequency Quadrupole (G) and the ALPI Linac (H). Such a highly energetic (up to 40 MeV), isotopically pure beam can be finally sent to the experimental hall for high energy nuclear physics experiments.

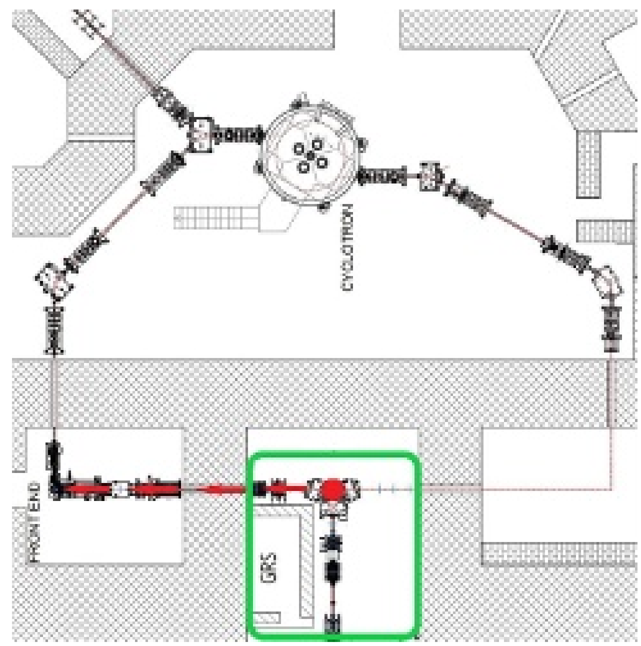

FIG. 2. Layout of the SPES building level-1; the green box represents the laser laboratory at level +1; the red dot represents the descending point for the laser beams while red arrows represents the laser beam path through the vacuum beamline to the ion source.

B. Laser Resonant Ionization in SPES Project.

One of the fundamental requests for the study of radioisotopes at ISOL facilities is the possibility of producing ion beams with minimum isobaric interference.

The most conventional mechanisms to ionize the desired nuclear reaction products are either the direct surface ionization[8] or the use of plasma ion sources[9].These tools have been suitably demonstrated, but they are chemically non-selective, in such a way that the cited goal cannot be always obtained. Therefore, in a relevant number of cases, many experiments could not be successfully designed and realized by employing these two techniques. The resonant laser ion source (LIS) overcomes this problem due to the typical features of laser-atom interaction as applied to the multi-step excitation of an atomic species beyond the ionization energy limit. The three ionization methods together with the elements of SPES interest are summarized in Fig. 3.

In a LIS, an atom can be ionized via three typical multi-photoionization schemes as shown in Fig. 4. In all the schemes the atoms are initially excited to a first discrete energy state well below the Ionization threshold, IP by the absorption of photons of wavelength λ_1. Then, in the various scenarios (from left to right) the absorption of a second photon of suitable energy causes, a) the transition to an autoionizing state located above the IP, and ionization is then achieved via non radiative energy transition of the electron to the continuous energy distribution above the IP, b) the direct ionization with the transition above the IP, c) the excitation to a high-lying Rydberg state close to the IP, from which ionization can be caused by thermal or electrical excitations.

The fundamental requirement of a laser ion source is the availability of tunable laser radiation able to match the fully resonant excitation of upper atomic levels in a range from UV (around 250 nm) to IR (close to 1.0 m), as will be discussed in par. IIB. Besides the large range of tuning, the spectral linewidth is an additional limiting parameter. In order to resolve between the energy levels of two different isotopes, spectral linewidth of the order of 100 MHz would be required. On the other hand the Doppler broadening due to temperatures of about 2000 C, typical of the environment in the target/reaction chamber and ion source, allows to relax this requirement to within 1-10 GHz range. At 2000 C, the effusion time for the atoms from the transfer line to the end of the hot cavity is approximated to 50-100 s. In order to have the presence of a photon flux during this time frame, a repetition rate of atleast 10kHz is required. Modern tunable laser sources can match these requirements and in addition can provide intensity values in the mW range (for the UV)up to several W (in the visible and IR) enough for step wise ionization of almost all the elements of the periodic table. The laser ion source is located at about 15-20 m from the output coupler of the laser and has an entrance window of about 3 mm. This asks for low laser beam divergence coupled with a proper opto-mechanical beam-steering system for the non-trivial stable overlapping of multiple laser beams, i.e. pointing stability better then 0.05 mrad.

The advantage of LIS is that the complexity of the ion source (the laser system) is at a radiation-safe distance from the high radiation environment. The challenge of element selectivity can be achieved inside the simple and inherently radiation-resistant cavity of the surface ion source. The method has been proved so efficient and convenient that it has been implemented in the most important RIB centers, as, for example, IRIS-PNPI, CERN-ISOLDE, TRIUMF-ISAC, GANIL, GSI, RIKEN, JYFL, KU Leuven, JG Mainz, in the past 15 years (see[10,11]). On account of the high degree of selectivity achieved, RILIS operation is requested by the users for thousands of hours per years.

C. Results of photionization in an offline lab at LNL

We report here a brief summary of the results of photoionization on four elements as obtained in an offline laboratory in LNL, on the stable isotopes, using an "old" laser system. We have completed measurements on aluminum, germanium and tin, while we have started an experimental study of silver. Selection of these elements has been driven by the interest of users in the SPES facility. In any of these specific cases, the preliminary step is the search for appropriate atomic lines according to the NIST database[12]. Resonance conditions are then studied in a HCL:Hollow Cathode Lamp, where the population redistribution among the atomic levels, caused by laser light irradiation, is evidenced by a change in the electric impedance of the discharge. This is known as the OGE:Opto-Galvanic Effect. In fact, HCLs are used in order to have a complete spectrum of a single element that is stored in the special shaped cathode, and is transferred in the vapor phase by a sputtering process in the

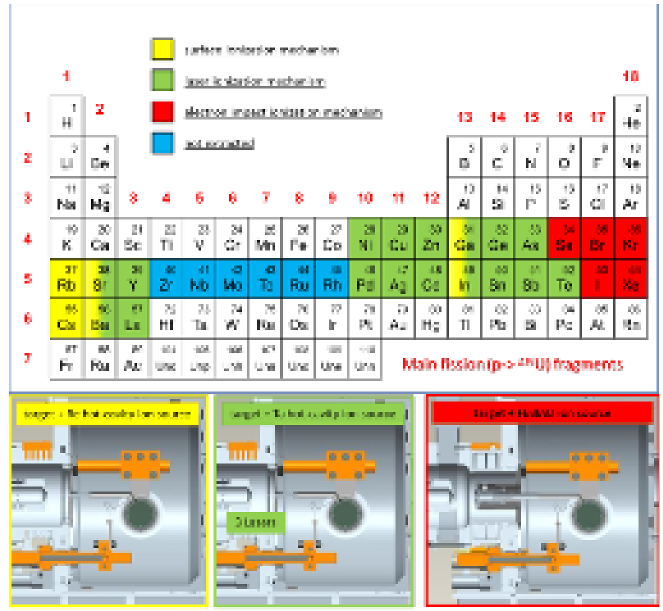

FIG. 3. Atomic elements produced by SPES facility and the ionization methods. Surface ion source in yellow, Laser ion source in green and plasma ion source in red.

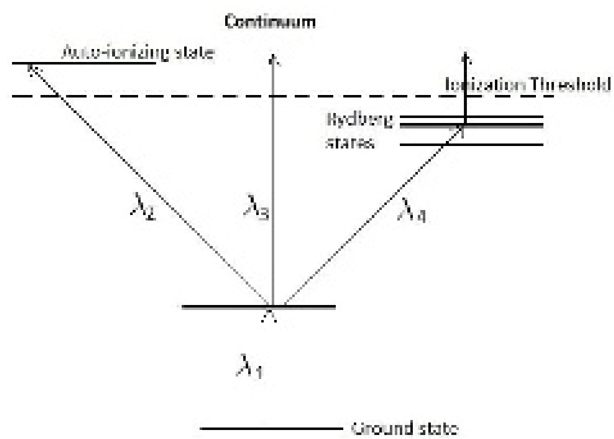

FIG. 4. Photoionization schemes.

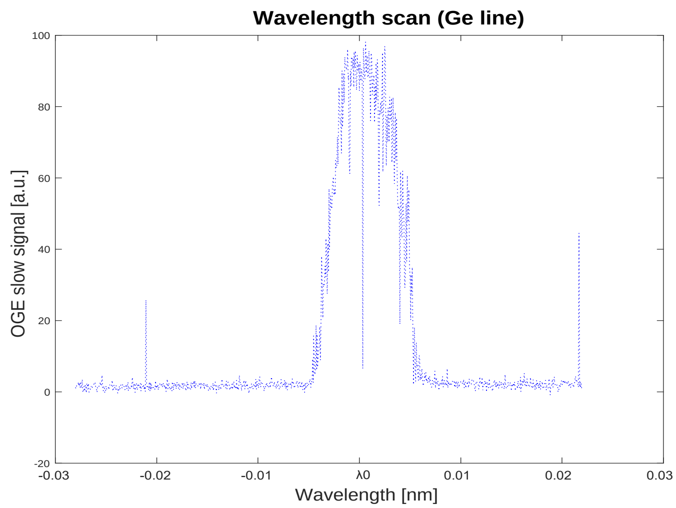

FIG. 5. Slow OGE Signal of germanium HCL collected with a scan of the Dye laser wavelength around the first transition level of Germanium ($\lambda_0 = 265.15683\,nm$ NIST line in air).

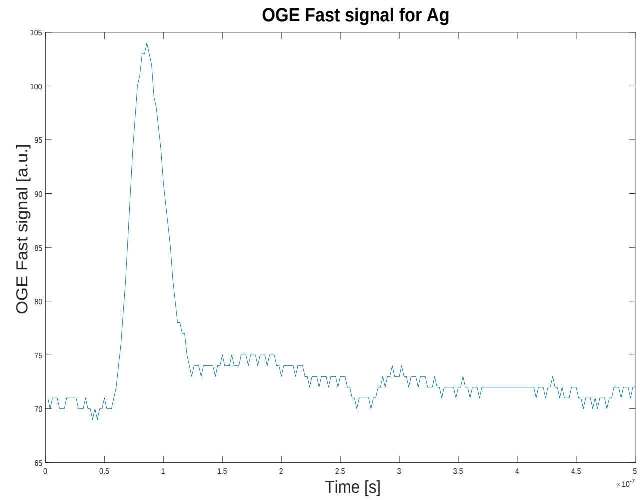

FIG. 6. Fast OGE Signal of silver HCL collected while the Dye laser is tuned to the first transition level of silver (NIST line $328.0680\,nm$ in air).

continuous discharge regime[13].

The typical response due to a monochromatic resonant single pulse is given by a "slow" dynamics, where the excitation of the 10-30 ns laser pulse is transferred to the gas mixture in the lamp consisting of the atomic species and a confining buffer gas in a time interval of the order of several microseconds. In this way, one can test the relative efficiency between the different steps in the excitation chain, having proof of the resonant condition by scanning the laser wavelength in order to obtain the line profile and verification of the saturation intensity values[14]. In reference [[14]], an example of saturation curve of the excitation steps has been reported. In Fig. 5, an example of a dye laser scan around the resonance frequency of a first step excitation in the case of germanium atom is shown. The signal is produced starting from the slow signal of a Ge HCL, as previously described.

The "fast" dynamic signal, characterized by a time duration of a few ns corresponds to the ionization process triggered by the laser pulse. This signal grows when the various laser exciting frequencies match the resonance conditions according to the scheme in Fig. 4.
In Fig. 6, a direct fast signal for the silver atom is presented. In this specific case, a high-lying Rydberg state very close to the IP, is populated via a double-photon absorption of a single color. It is the first evidence in our offline lab for the successful photionization of silver, one of the most important elements for the application in radiopharmacy for the SPES project and its applied branch ISOLPHARM[15]. Further studies on silver will be performed using HCL and Time of flight mass spectrometer.

HCL has also been used to test different ionization schemes on the same atom, in order to select the most efficient one[14]. For example, the eventual previous choice of a single color ionization gives a lower ionization rate, if compared with a different multistep scheme. In order to complete the preliminary experimental tests, a home built TOFMS:Time Of Flight Mass Separator has been used to detect the ions distinguishing among different isotopes. The vapor phase for the element to be studied is produced in a UHV chamber by an ablation laser, impinging on a solid sample. The generated plasma plume is confined in a cone of small angle guiding the ablated material by a chimney.

The ions are created by the multistep laser excitation in a small volume over the target, at the center of the electrostatic system. Two electrodes and a grid are used to accelerate and focus these ions. The ion collimated beam, after a free flight of 2 m linear path in a high vacuum tube, arrives on a MCP:Multi Channel Plate detector. The Simion[16] software allows us for a modelling and a prediction of the possible trajectories of ions in the electric field and in the free flight zones, as a function of the electrode voltages and of the ionization point/volume above the target. In Fig. 7, the MCP signal for Al is shown: the ions appear after around 15.5 s, as predicted by the calculations. Again, if we scan the ionization laser (a single color is enough in order to ionize the atom), we can obtain the line profile (see Fig. 8).

In presence of a mixture of different isotopes, the laser ionization method associated to TOF reveals itself as an excellent Mass Spectrometry tool, as demonstrated by the tin signal shown in Fig. 9 where the signals corresponding to the different isotopes according to their natural abundance is detected after ionization. A detailed description of our TOF-MS and tin laser resonant ionization experiment has already been published by our group[17].

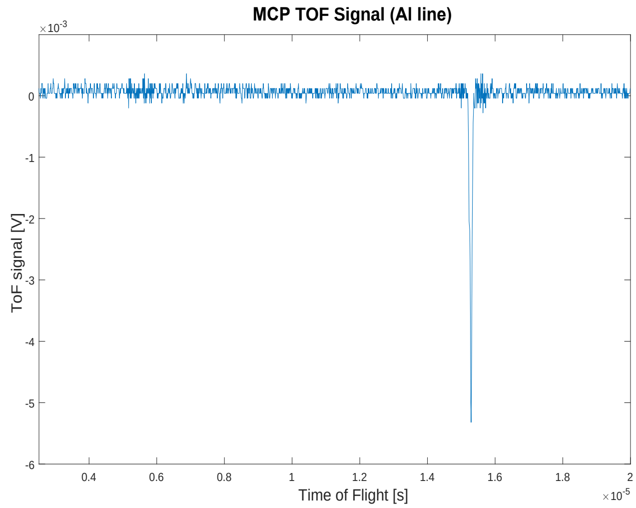

FIG. 7. Time of Flight MCP signal of Al ions.

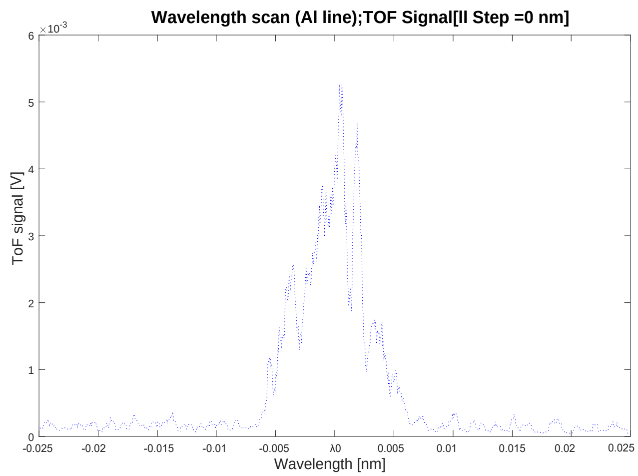

FIG. 8. Wavelength scan of Al ions MCP signal centered on $\lambda_0 = 308.21529\,nm$ NIST line.

II. NEW TISA TUNABLE LASER SYSTEM

The requirements for the laser systems are essentially, wide tuning range, to span the largest possible combination of wavelengths according to the complex levels structure of candidate elements, short pulse duration of the order of a few tens of ns, in order to comply with the short life-time of excited energy levels, high repetition rate and relatively high power to guarantee a high ionization rate.

In principle, the modern laser technology offers fundamentally two possible candidates for the ionization goal in a LIS facility: dye lasers, as used in our offline lab, and TiSa lasers. Solid state technology is confirmed to be the preferred choice in terms of reliability and practical management[11,18–20]. In fact, this kind of solution is preferable for maintenance during activities, possibility of long term stable operating system and fire-hazard risk reduction. The new SPES laser system has been bought by INFN in an international tender[21]. It consists of:

- 3 individual pump lasers (*Spectra-Physics Ascend*)
- 3 individual TiSa units (*Sirah Credo-TiSa*-10 kHz)
- 2 High Harmonic generation units (*Sirah HHG*)
- 1 synchronization system (*Quantum*)
- 1 Wavemeter (*Toptica WS7*)
- 4 beam pointing stabilization system (*Aligna*®)

as provided by Laser Optronic and Sirah companies.

A. Pump Lasers.

The Pump lasers (Spectra-Physics Ascend) have been chosen by Sirah and the TiSa lasers have been directly designed in order to be optimized with this model. At its maximum current each pump laser can deliver more than 50 W emitting 527 nm light in 50 ns pulses at 10 kHz repetition rate. In Fig. 10, the curve of pump average power measured directly at the exit of each laser varying the diode current is shown. The measurement was performed with a *Ophir NovaII*® coupled to a *F150-bb-sh-26* head.

The third laser, evidencing a lower power, is 2 years older than the other ones, as it has been used to design, test and optimize the first prototype of the TiSa laser. This does not have major consequences on the overall performance of the system.

B. TiSa Lasers.

The TiSa laser has been specifically developed in order to satisfy the SPES technical requests. The main TiSa laser system parameters are listed in Table I. It is an upgraded evolution of a previous commercial laser, with an innovative design. The active medium is given by two TiSa crystals, instead of a single one, in a geometry for the pump power beam propagation that allows for an optimization of the waist and a significant increase in the output power. Details of the laser oscillator design are in Fig. 11. The pump beam is split in two symmetrical beam arms and reaches the two crystals passing through a focusing lens. The optical TiSa cavity is “Z” shaped. The tunable system is based on a birefringent optics mounted onto an automated motion stage. To optimize power for a large wavelength range, one of the cavity end-mirror can be chosen from a mirror triplet lodged from a selection stage. In order to ensure the synchronization of the three Ti:Sa lasers, each pumped by a separate green laser, an intracavity

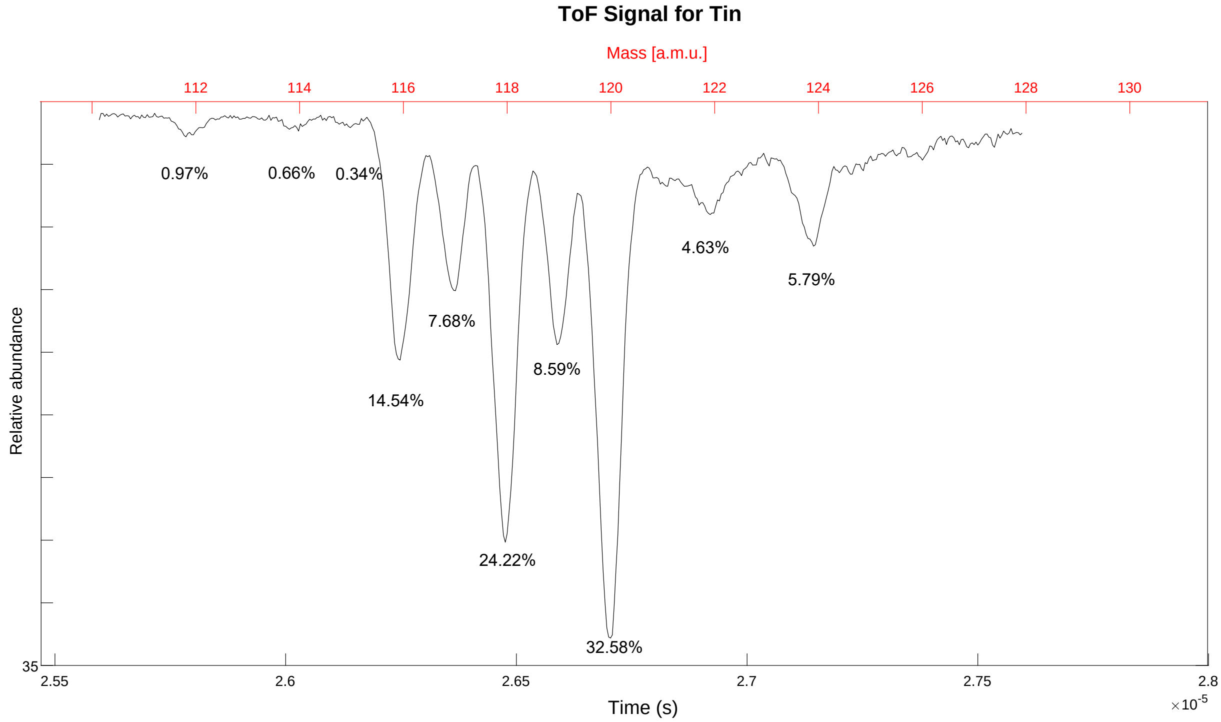

FIG. 9. Time of Flight MCP signal of a natural mixture of Sn isotopes.

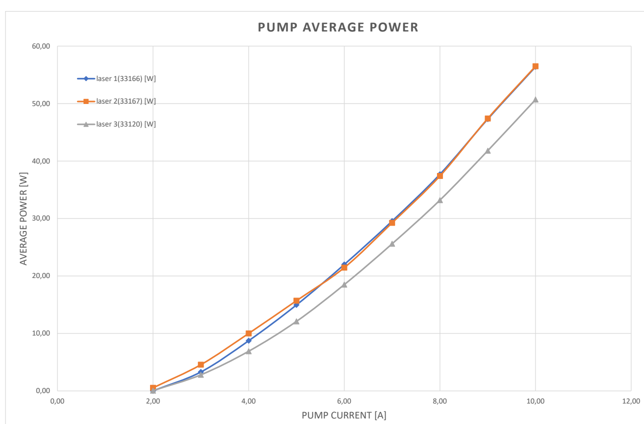

FIG. 10. Average pump power vs diode current @ $10\,kHz$ repetition rate.

TABLE I. Table of main laser system parameters.

Parameter	Value
Pump Repetition Rate	$10\,kHz$
Pump Power	$57\,W$
Tuning Range	$690-950\,nm$
Pulse Duration (τ_{FWHM})	$30-50\,ns$
Repetition Rate	$10\,kHz$
Output Power (λ_{Peak}@$10\,kHz$)	$6,8\,W$
Line-width	$< 6\,GHz$ (One Etalon)
Beam divergence	$< 1,5\,mrad$
Beam diameter	$1\,mm$ Typ.

Pockel's cell is mounted. To fulfill narrower bandwidth requirements, a double intracavity etalon system can be installed. Finally, each TiSa unit has its own controller and an optical fiber coupling to read wavelength with a WS7 lambda-meter.

C. New laser laboratory.

The SPES facility was planned to have two radioactive ion beam target stations into two different bunkers. The laser laboratory position into the building is thus optimized to serve them both, minimizing distances as much as possible. The laboratory is placed at level +1, just on the top of the combiner magnets room (Fig. 2). The laser beam goes, by means of a hole in the lab floor, to the center of the combiner magnets and can reach each bunker entering in the beam line pipe using the vacuum viewport access in each magnet chamber. Fig. 12 represents the laboratory design layout, its dimensions and principal furniture. The laboratory has been designed in order to prevent dust contamination inside and to keep the main room as clean as possible. The main area (*LABORATORIO LASER L2* in Fig. 12) is accessible by means of a dressing room (indicated as *SPOGLIATOIO L1* in the picture). Light over-pressure air is kept in all the laboratory (L2 on + 60 Pa and L1 at +30 Pa) to avoid dust contamination from the external environment. The air conditioning system ensure ±1° C temperature stabilization and laminar air flux on each table is provided by filtering hoods on the roof. By this design it is possible

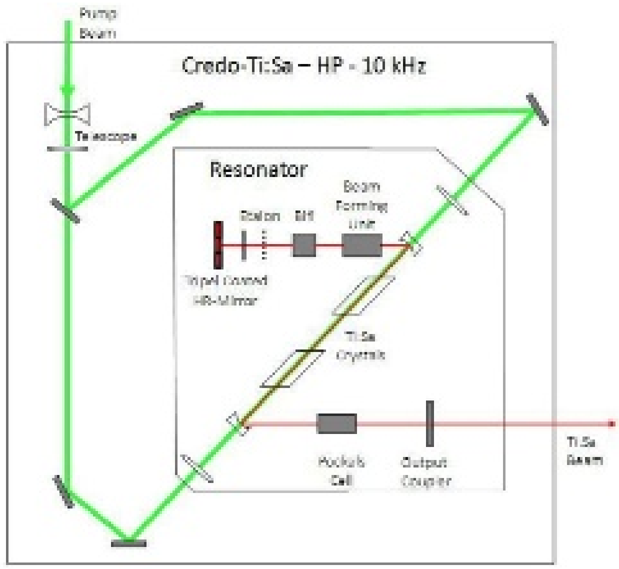

FIG. 11. Optical layout of the Sirah TiSa system.

to have and maintain ISO8 Class for the main room. The internal layout laboratory assigns two 1500 x 2400 mm^2 optical tables, connected in reverse "L-shape" configuration, to the main laser system, the beams combination optics and the beam position monitors. The third optical table is foreseen for future developments and it is actually used as measuring station for in-lab experiments. The connection of the laboratory to level 0 is ensured by a hole in the floor sealed with DIN600 vacuum standard flange to maintain over-pressure. Once the laser beam path will be definitive, the flange will be machined with proper small hole to minimize the outlet. Regarding laser safety each pump laser is connected by its interlock port to the laboratory door controller circuits. Access to the lab is granted by keypad combination door-lock system to prevent unauthorized access while upon every incorrect exit procedure the lasers are shut down.

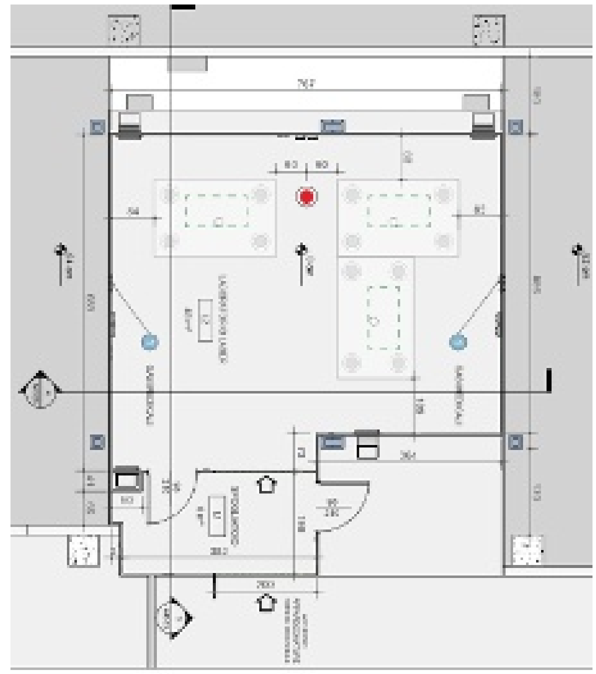

FIG. 12. Design of the new lab[22]; the red dot represents the descending point for the laser beams.

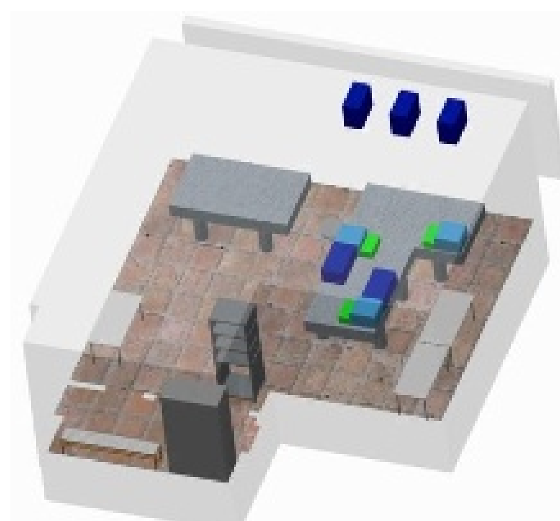

FIG. 13. Conceptual 3D laboratory design with three laser systems. The pumps, Tisa and harmonic stages are indicated as the green, sky blue and classic blue boxes respectively on the L-shape optical table. The chillers (dark blue box on the roof), spare optical table and furnitures are indicated as well.

D. Laser installation and commissioning.

During late 2018, the installation of the new laser system has begun. The optical tables were inserted before the laboratory main walls were finished. For future possible installation into the laboratory, a portion of the L1 and L2 walls is still movable. The main power for laser power controllers and water from the chillers are connected from below the optical tables in order not to interfere with other systems and cables. The 3 chillers for pump lasers are outside the laboratory to minimize the noise in the lab environment.

In Fig. 13, a 3D design of the laboratory is presented. It is possible to see laser disposition on the optical tables: green is for pump lasers, sky blue for the TiSa units, in classic blue for the high harmonic generation units. On the top of the laboratory in dark blue are the three chillers.

TABLE II. Table of TiSa laser M^2 measures.

Laser Stage	TiSa1	TiSa2	TiSa3
Fundamental	4.14	4.5	3.04

III. LASER PERFORMANCES

During the commissioning phase several laser performances were tested as requested in the tender acceptance tests. These performances are among the ones of paramount interest for the SPES project. After the commissioning, more intensive tests were conducted to probe different laser parameters using different techniques[23]. The results are described in the following sections.

A. Power.

Power measurements were performed at several wavelengths of interest. For each data-set, a procedure for optimizing the cavity performances was applied. It consists of output-coupler and pump beam mirrors alignment adjustment for the TiSa units and crystal angle tuning and mirrors alignment adjustment for high harmonic generation stages. In Fig. 14, the corresponding power curves for one of the three TiSa lasers are reported, including also the response of the high harmonic generation stages. The experimental points have been obtained for 51 W pump power.

B. M^2 Parameter.

One of the most important features for defining the quality of a laser beam is the M^2 parameter; it gives a quantitative indication of the possibility of a good focusing and of the laser beam propagation[24]. The beam quality factor M^2 can be calculated with a fitting procedure, applied to the measured evolution of the beam radius along the propagation direction[25]. In order to easily measure M^2, we built an automated two linear axis movement stage to perform a knife edge technique. In Fig. 15, a fitted measurement of M^2 parameter for one of the three TiSa lasers is reported. The other two systems give similar behaviors and values. The power measurements for the fitting procedure were performed with a *Ophir NovaII®* coupled to a *F150A-BB-26* head.

C. Pointing Stability.

The laser beam position stability on target affects directly the produced ion beam current variation in time. This aspect can be easily explained considering a well collimated laser beam entering directly into the ion source tube: in SPES, it is a 30mm long tube with 3mm entry hole[8]. In the case of a correct and ideal alignment, the overlap between the ionization volume and the laser beam is maximum and matches the inner hollow cylinder volume of the ion source. In the presence of any misalignment, this overlap volume is reduced, a smaller interaction region for atoms and photons is defined and the ion production rate decreases. Any variation in time of this interaction volume produces a variation in time of the ion current. Therefore, the more the laser beam is stable, the less instabilities of beam current occur. In the designed SPES building the total laser beam path to the ion source is approximately 20 m: the first 10 m are travelled in air and the last 10 m inside the vacuum line. The entrance window in the vacuum line will be at level -1 in front of the first part of the bending magnet as shown in Fig. 2.

In order to fulfill the requirements of the best beam pointing stability, the whole laser system included an automatic beam positioning control system by Aligna as mentioned in Section II. The Aligna system native configuration, is composed by:

a) 2 actuated (galvo+stepper motors) mirrors mounting (**M**), mirrors according to wavelength requests;

b) 1 beam sampler (**BS**) according to wavelength requests;

c) 1 multiple position detector (**D**) according to wavelength requests;

d) 1 laser diode source (**L**) for demo tests;

e) 1 target (**T**) for demo tests;

f) 1 electronic controller, able to control 2 optical sets.

g) precision stability well below 1 μrad

At the moment, due to the work in progress in the preparation of the furniture of the SPES building, it is not possible to place any optical components at the level -1 of the target and ion source. Therefore it is not possible to perform any laser beam pointing stability test using the final configuration. To overcome this impasse, an alternative laser beam path was designed using the third optical table in the laser laboratory as shown in Fig. 16. Four 2 inch mirrors have been mounted facing each other at 2 m distance; using multi-reflection of the laser beam it is possible to emulate the double 10 m section to simulate the real laser beam path. Mirrors and detectors of the Aligna system are placed in this dummy setup according to the real distances in the final configuration. This test setup has demonstrated the possibility to strongly reduce the mechanical noise. The result is shown in Fig. 17, where the traces indicate the laser position with respect to the set point as a function of time in absence of the servo stabilization. The feedback loop is turned ON and OFF to compare the two situation. The same measurements have been done several times

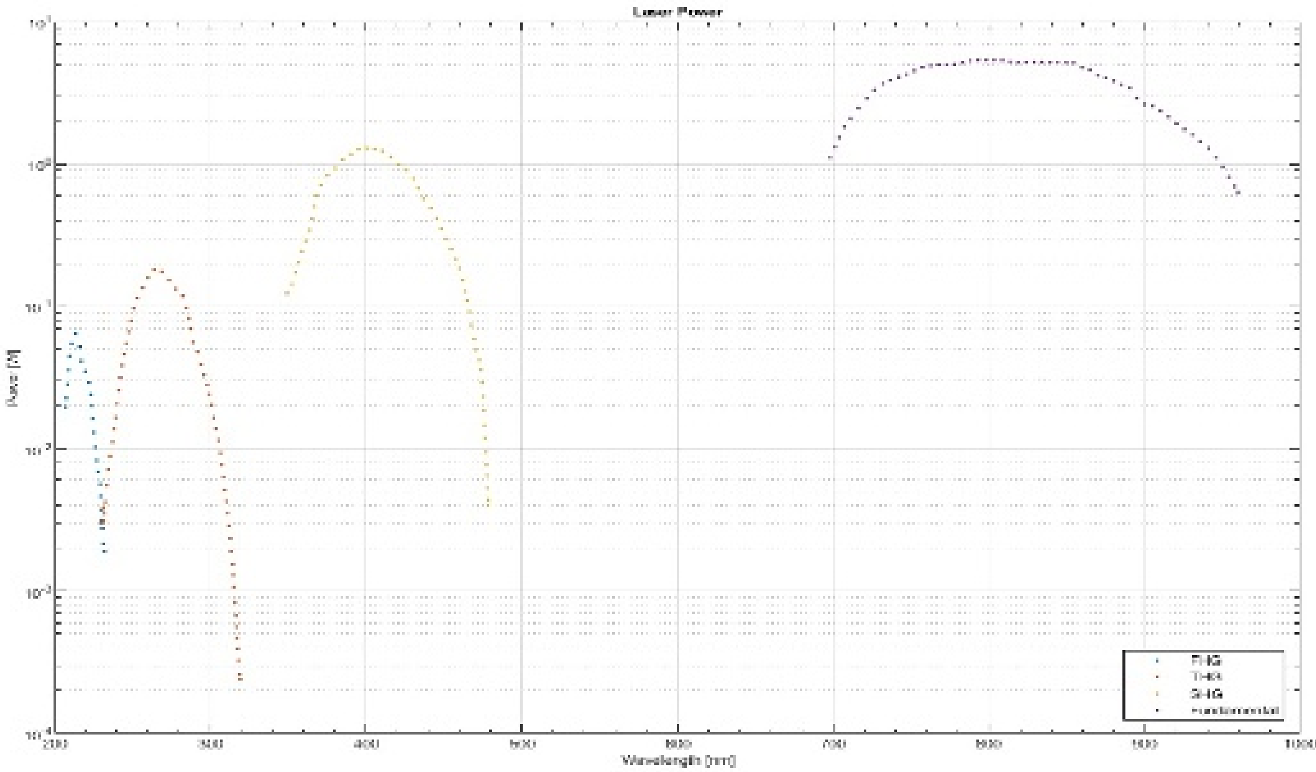

FIG. 14. Power measurements of TiSa (Laser 3 in Fig. 10) vs wavelength; fundamental and higher harmonic outputs at pump power of 51W.

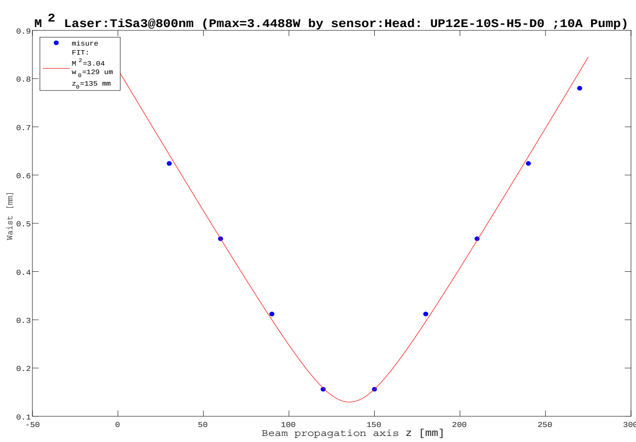

FIG. 15. Measured M^2 and fitting curve for one of the three TiSa laser.

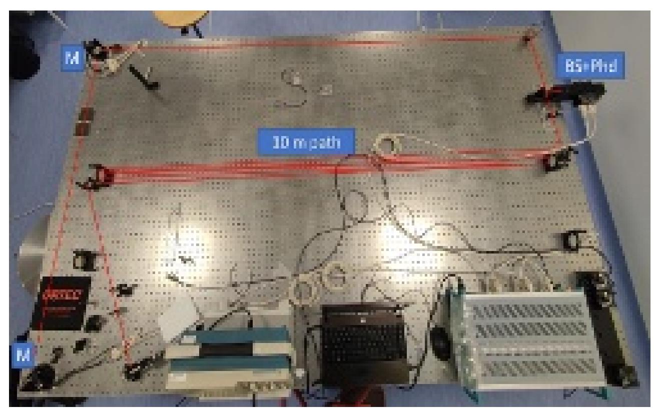

FIG. 16. Aligna system optical components in our demo configuration: M - mirror including piezo-actuator, BS - Beam sampler and photodiodes, 10m multiple reflection and observation point at the end of the path, laser beam path simplified in red.

for several hours showing a good stability of the system. Further detailed measurements are planned.

IV. CONCLUSIONS.

We have reported in this paper the recent efforts of the SPES project of INFN with special attention to the progress of the construction of a new Laser Ionization facility. We have discussed the status of the new Laser Lab and the measurements that have been performed as a preparation to the needs of the users, as expressed by specific Letters of Intent. The Laser group has used Hollow Cathode Lamps and a Time of Flight Mass Spectrometer in order to demonstrate on stable isotopes the

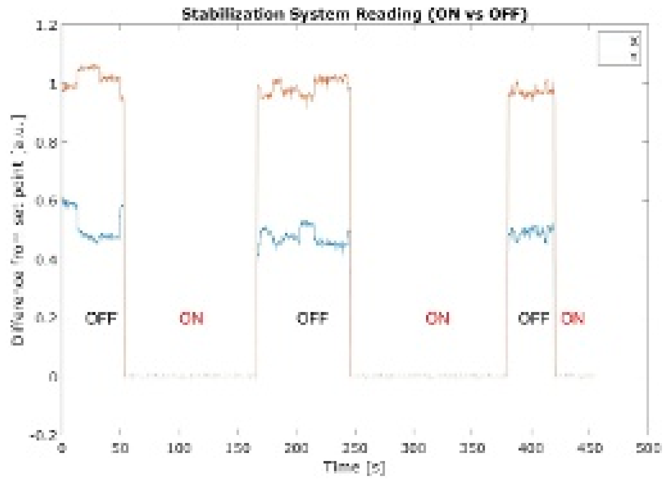

FIG. 17. Stabilization system feedback signals, X horizontal and Y vertical direction. The feedback loop is turned ON and OFF to compare the two situation.

ability of ionizing different elements of interest (Al, Ge, Sn, Mo, Ag), as well as separating different isotopes in a natural mixture. In the final online lab, a new version of the TOFMS will be installed in the next few months, while the specific parameters characterizing the new laser systems have been measured.

V. ACKNOWLEDGMENTS

Authors wish to thank Andrea Calore for the precious help in all laboratory needs addressed to the technical division and the managing the laser laboratory environmental system during each phase of the activity.
Authors wish to thank Silvano De Pascalis from LaserOptronic and Paulus Jauernik from Sirah Lasertechnik for the hard work during all this years of *R&D*, construction, installation and testing.
Authors have to thank Alessandra Tomaselli for her presence in our group since the very first moment: there wouldn't have been any group, lasers or laboratories without. Her premature departure leaves an immense void. Alessandra's wisdom, kindness, humanity and help will be forever missed.

VI. DATA AVAILABILITY

The data that support the findings of this study are available from the corresponding author upon reasonable request.

[1] Y. Blumenfeld, T. Nilsson, and P. V. Duppen, "Facilities and methods for radioactive ion beam production," Physica Scripta **T152**, 014023 (2013).
[2] M. Durante and K. Parodi, "Radioactive beams in particle therapy: Past, present, and future," Frontiers in Physics **8**, 326 (2020).
[3] I. Tanihata, "Nuclear physics with rib's: How it all started," The European Physical Journal Plus **131**, 90 (2016).
[4] F. Hammache and N. de Séréville, "Transfer reactions as a tool in nuclear astrophysics," Frontiers in Physics **8** (2021), 10.3389/fphy.2020.602920.
[5] F. Gramegna, P. V. Duppen, A. Vitturi, and S. Pirrone, *Nuclear Physics with Stable and Radioactive Ion Beams* (Ios Pr Inc, 2019).
[6] G. Prete, "The SPES project at the INFN-Laboratori Nazionali di Legnaro," Nuovo Cim. C **38**, 181 (2016).
[7] G. Prete, A. Andrighetto, J. Esposito, P. Mastinu, and J. Wyss, "The spes project: a second generation isol facility," Physics Procedia **26**, 274–283 (2012), proceedings of the first two meetings of the Union of Compact Accelerator-Driven Neutron Sources.
[8] M. Manzolaro, F. D'Agostini, A. Monetti, and A. Andrighetto, "The SPES surface ionization source," Review of Scientific Instruments **88** (2017), 10.1063/1.4998246.
[9] M. Manzolaro, "Ongoing characterization of the forced electron beam induced arc discharge ion source for the selective production of exotic species facility," Review of Scientific Instruments (2014).
[10] S. Rothe, T. D. Goodacre, D. Fedorov, V. Fedosseev, B. Marsh, P. Molkanov, R. Rossel, M. Seliverstov, M. Veinhard, and K. Wendt, Nuclear Instruments and Methods in Physics Research B **376** (2016), 10.1016/j.nimb.2016.02.024.
[11] V. N. Fedosseev, Y. Kudryavtsev, and V. I. Mishin, "Resonance laser ionization of atoms for nuclear physics," Physica Scripta **85** (2012), 10.1088/0031-8949/85/05/058104.
[12] U. D. of Commerce, "National institute of standards and technology," (2009).
[13] D. Butcher, "Encyclopedia of Analytical Science (Second Edition)," (2005).
[14] D. Scarpa, A. Barzakh, D. Fedorov, A. Andrighetto, E. Mariotti, P. Nicolosi, and A. Tomaselli, Review of Scientific Instruments , 02B708.
[15] F. Borgna, M. Ballan, C. Favaretto, M. Verona, M. Tosato, M. Caeran, S. Corradetti, A. Andrighetto, V. Di Marco, G. Marzaro, and N. Realdon, "Early evaluation of copper radioisotope production at isolpharm," Molecules **23** (2018), 10.3390/molecules23102437.
[16] L. (c) 2003-2021 Scientific Instrument Services (SIS) by Adaptas Solutions, "Simion - the industry standard in particle optics simulation software," (2021).
[17] D. Scarpa, D. Fedorov, A. Andrighetto, E. Mariotti, P. Nicolosi, L. Sottili, A. Tomaselli, R. Cecchic, and L. Stiaccini, "ToF diagnostic of Tin resonant laser photoionization in SPES laser offline laboratory," Journal of Instrumentation **11** (2016), 10.1088/1748-0221/11/09/C09001.
[18] S. Rothe, B. A. Marsh, C. Mattolat, V. N. Fedosseev, and K. Wendt, "A complementary laser system for ISOLDE RILIS," Journal of Physics: Conference Series **312** (2011), 10.1088/1742-6596/312/5/052020.
[19] J. Lassen, P. Bricault, M. Dombsky, J. P. Lavoie, C. Geppert, and K. Wendt, "Resonant ionization laser ion source project at TRIUMF," Hyperfine Interactions **162**, 69–75 (2005).
[20] A. Nieminen, I. D. Moore, J. Billowes, P. Campbell, K. T. Flanagan, C. Geppert, J. Huikari, A. Jokinen, T. Kessler, B. Marsh, H. Penttilä, S. Rinta-Antila, B. Tordoff, K. D. Wendt, and J. Äystö, "Laser ion source project at IGISOL," Hyperfine Interactions **162**, 39–43 (2005).
[21] INFN, "Bando di Gara "Sistema laser del progetto SPES"," Delibera GE 10583 del 16.01.2015 (2015).
[22] AAVV, "Gara per "Fornitura con posa in opera di una struttura tipo "camera bianca" per il laser del progetto SPES"," (2018).
[23] P. Rüdiger, "RP Photonics," (2004).
[24] A. E. Siegman, "Defining, measuring, and optimizing laser beam quality," in *Laser Resonators and Coherent Optics: Modeling,*

Technology, and Applications, Vol. 1868, edited by A. Bhowmik, International Society for Optics and Photonics (SPIE, 1993) pp. 2–12.

[25]ISO-11146, "Lasers and laser-related equipment – Test methods for laser beam widths, divergence angles and beam propagation ratios," (2005).

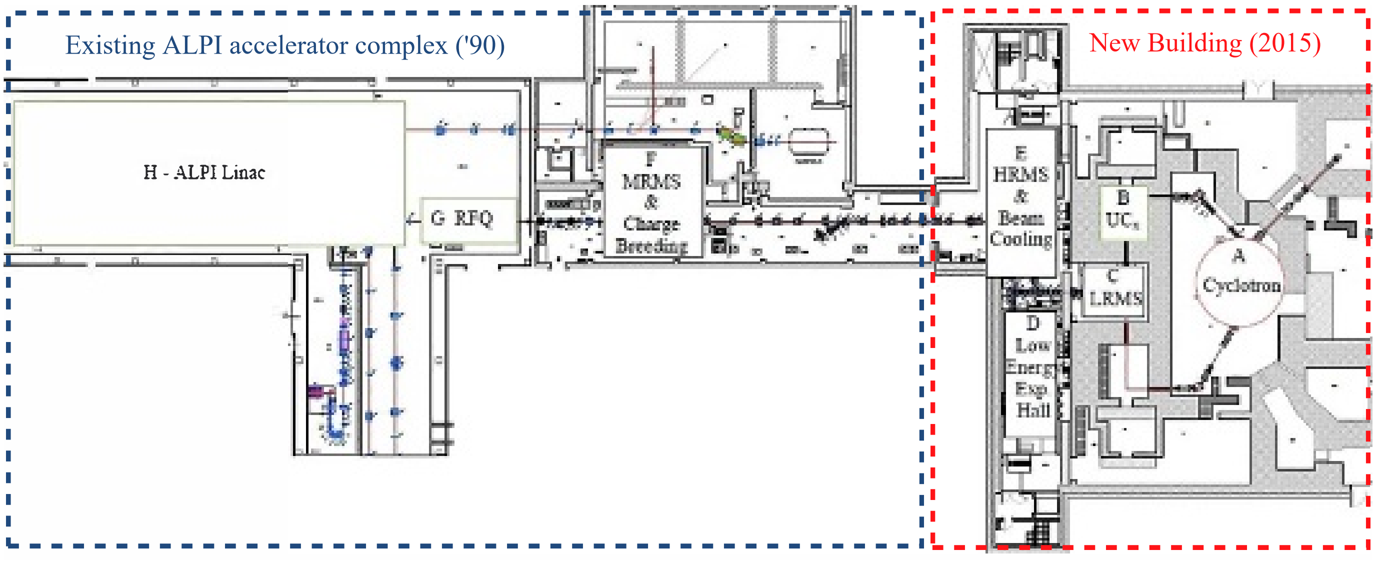

Existing ALPI accelerator complex ('90)
New Building (2015)
H - ALPI Linac
G RFQ
F
MRMS
&
Charge
Breeding
E
HRMS
&
Beam
Cooling
B
UC$_x$
C
LRMS
A
Cyclotron
D
Low
Energy
Exp
Hall

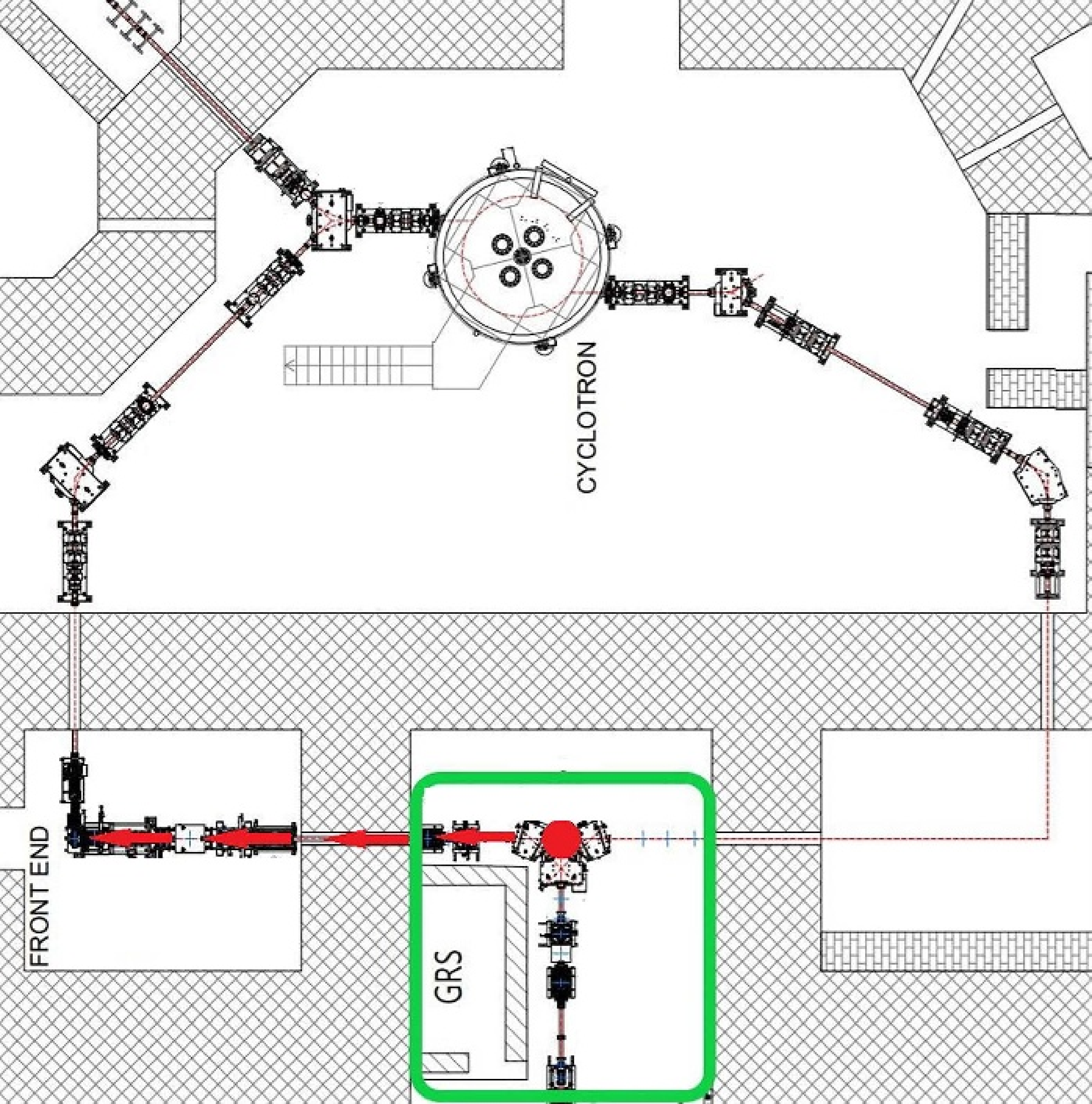
CYCLOTRON
FRONT END
GRS

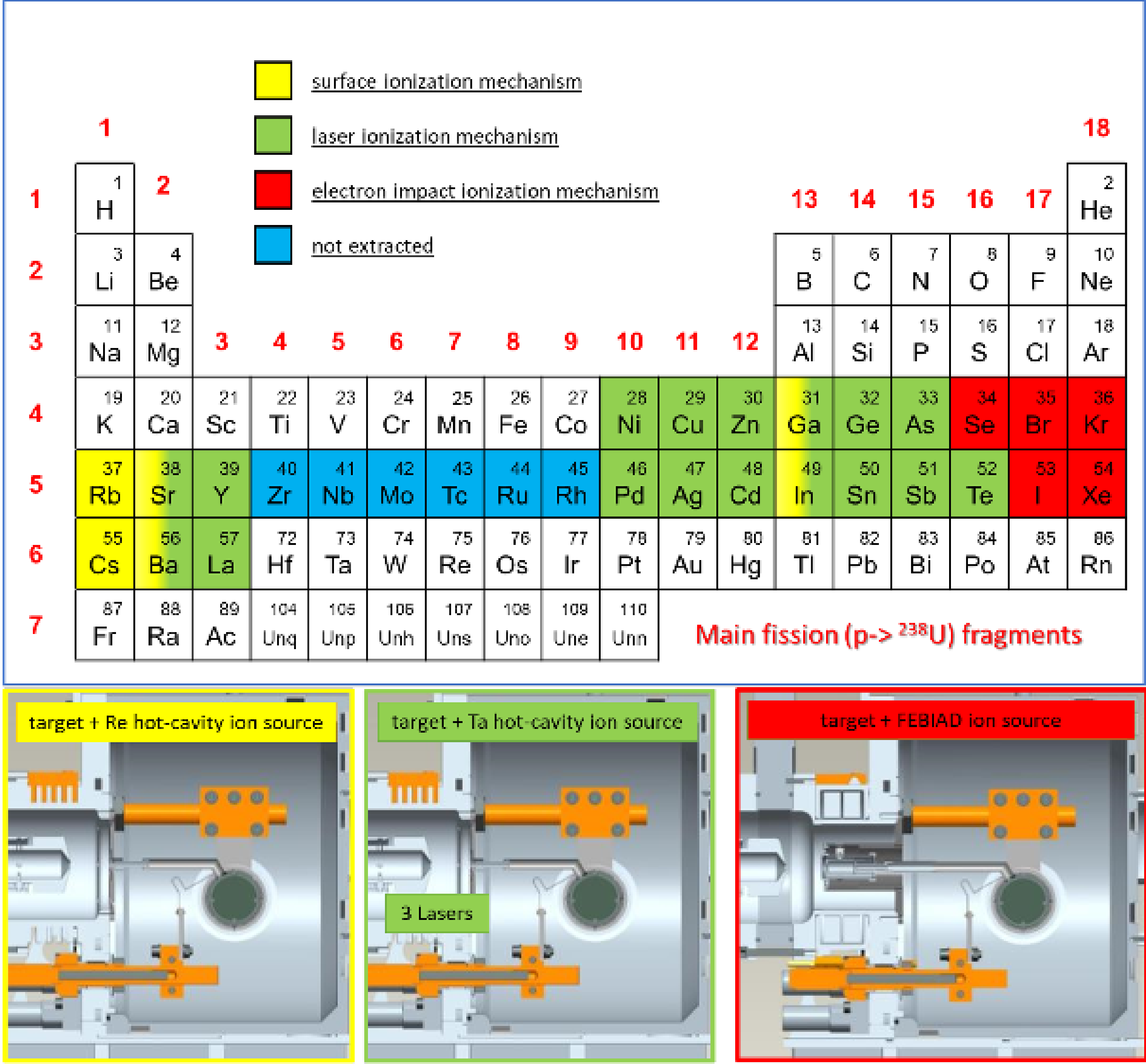

surface ionization mechanism
laser ionization mechanism
electron impact ionization mechanism
not extracted
Main fission (p-> 238U) fragments
target + Re hot-cavity ion source
target + Ta hot-cavity ion source
3 Lasers
target + FEBIAD ion source

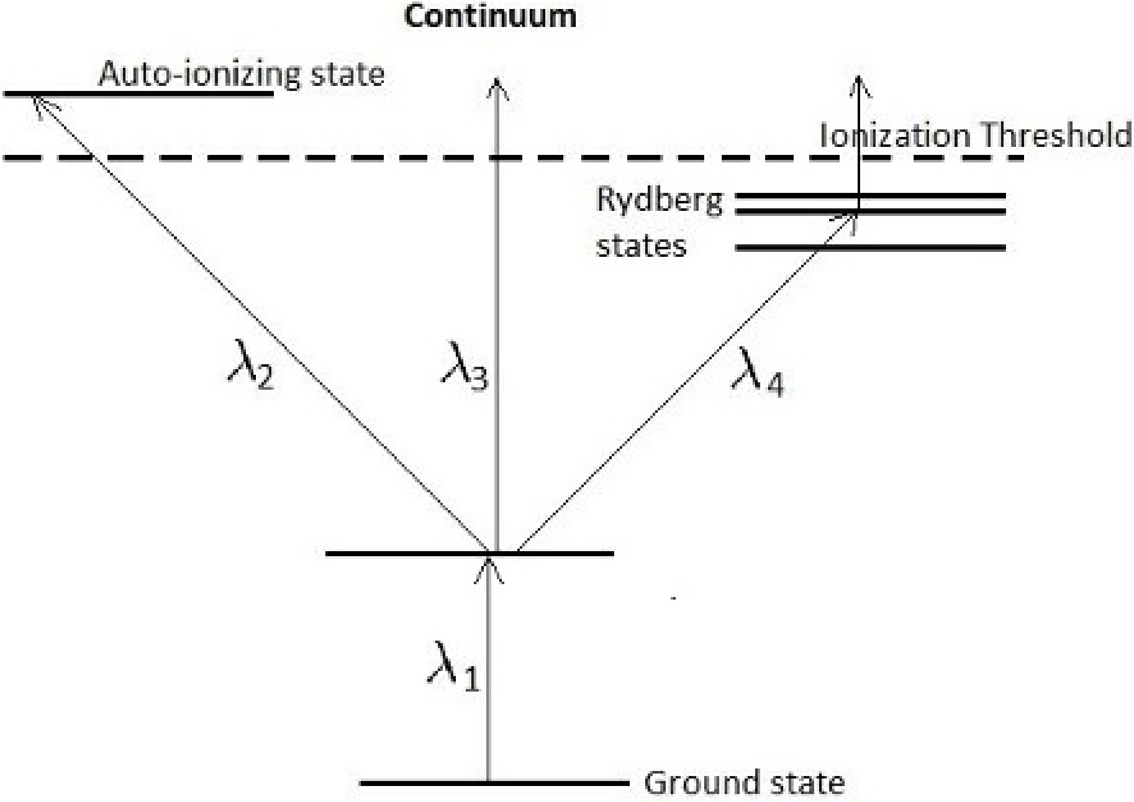
Continuum
Auto-ionizing state
Ionization Threshold
Rydberg
states
λ_2
λ_3
λ_4
λ_1
Ground state

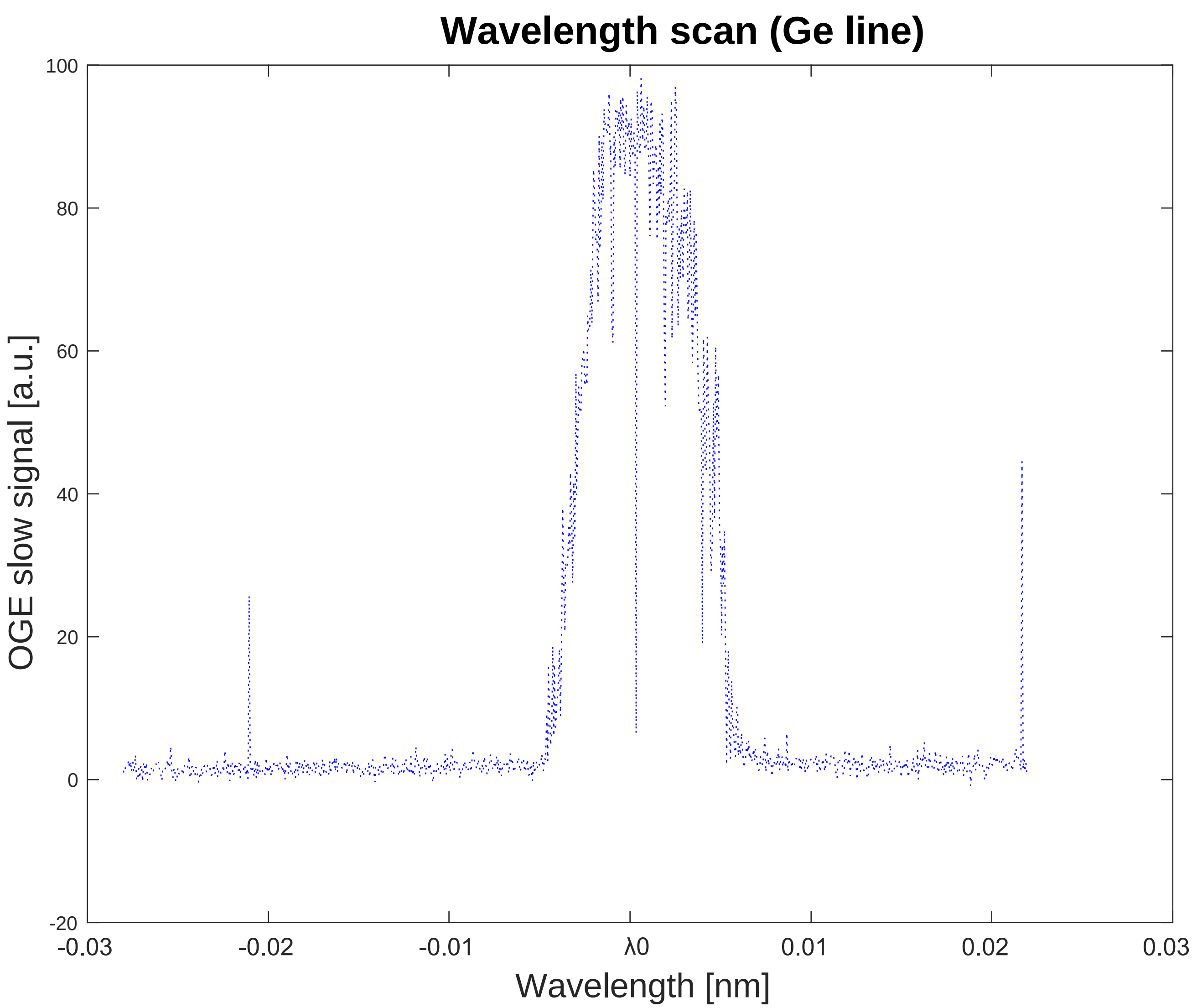
Wavelength scan (Ge line)
OGE slow signal [a.u.]
Wavelength [nm]
100
80
60
40
20
0
-20
-0.03
-0.02
-0.01
λ0
0.01
0.02
0.03

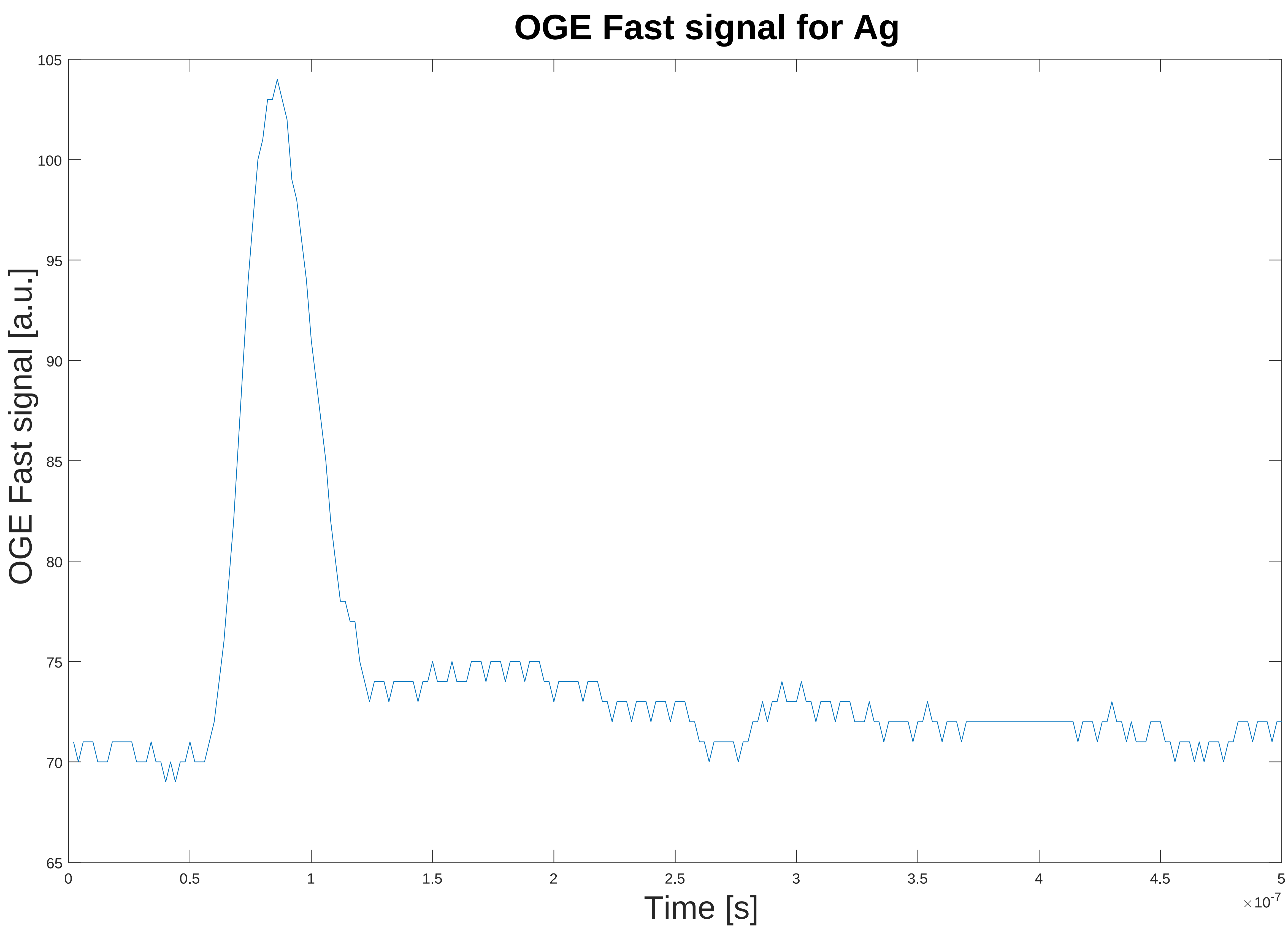
OGE Fast signal for Ag
OGE Fast signal [a.u.]
Time [s]
105
100
95
90
85
80
75
70
65
0
0.5
1
1.5
2
2.5
3
3.5
4
4.5
5
×10^-7

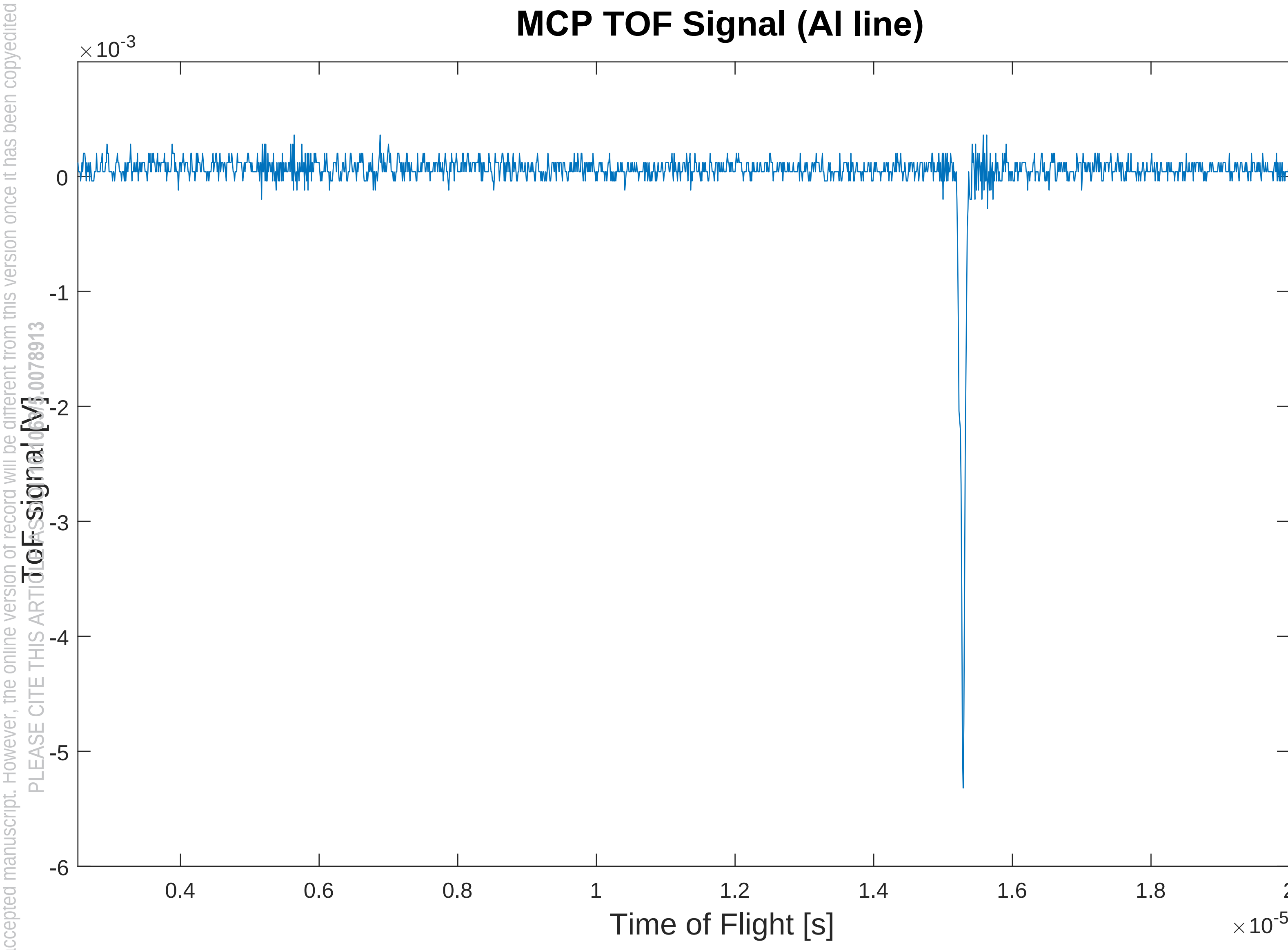
MCP TOF Signal (Al line)
×10^-3
0
-1
-2
-3
-4
-5
-6
ToF signal [V]
0.4
0.6
0.8
1
1.2
1.4
1.6
1.8
2
Time of Flight [s]
×10^-5

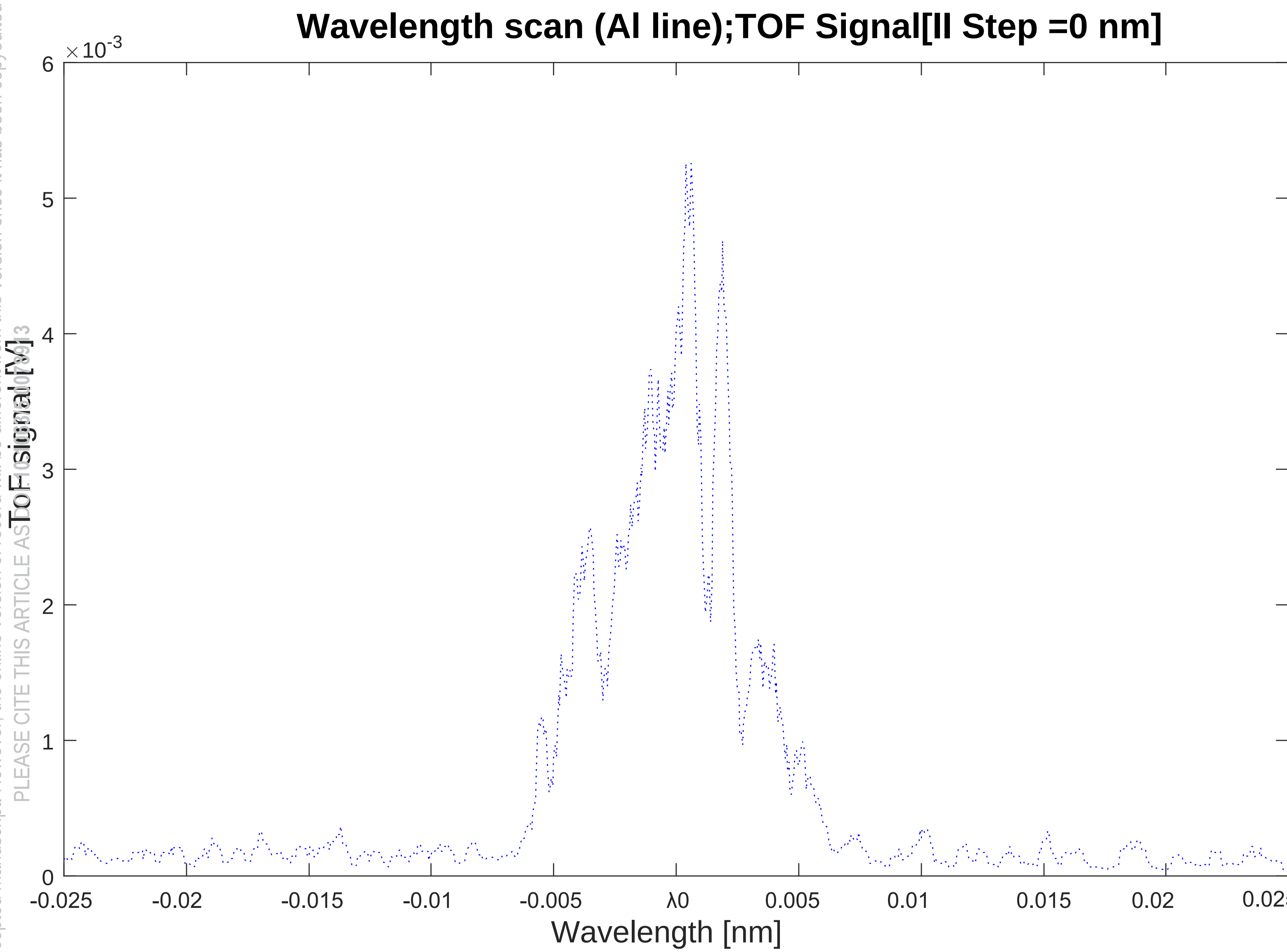
Wavelength scan (Al line);TOF Signal[Il Step =0 nm]
×10-3
6
5
4
3
2
1
0
ToF signal [V]
-0.025
-0.02
-0.015
-0.01
-0.005
λ0
0.005
0.01
0.015
0.02
Wavelength [nm]

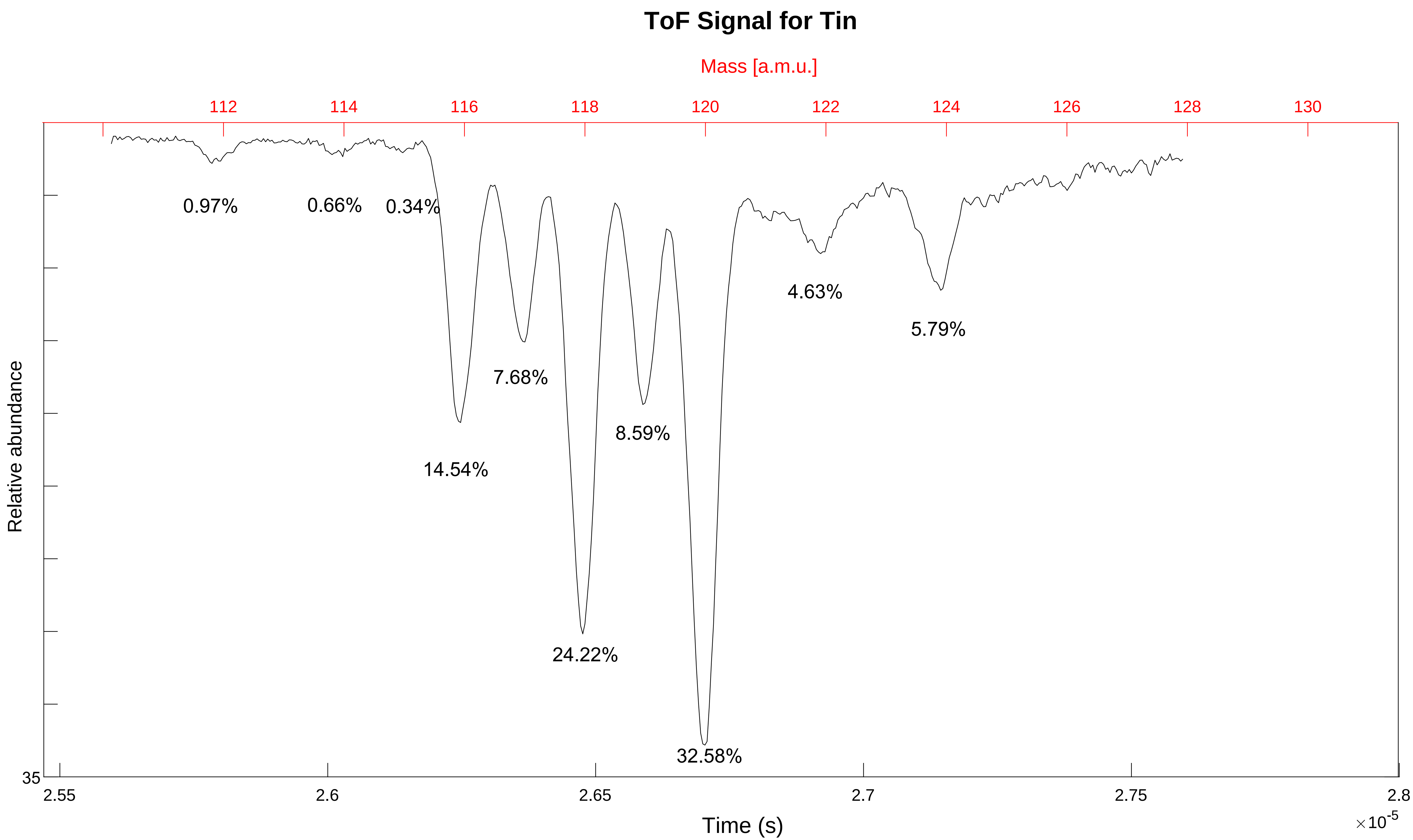

ToF Signal for Tin
Mass [a.m.u.]
112
114
116
118
120
122
124
126
128
130
0.97%
0.66%
0.34%
14.54%
7.68%
24.22%
8.59%
32.58%
4.63%
5.79%
Relative abundance
35
2.55
2.6
2.65
2.7
2.75
2.8
Time (s)
×10-5

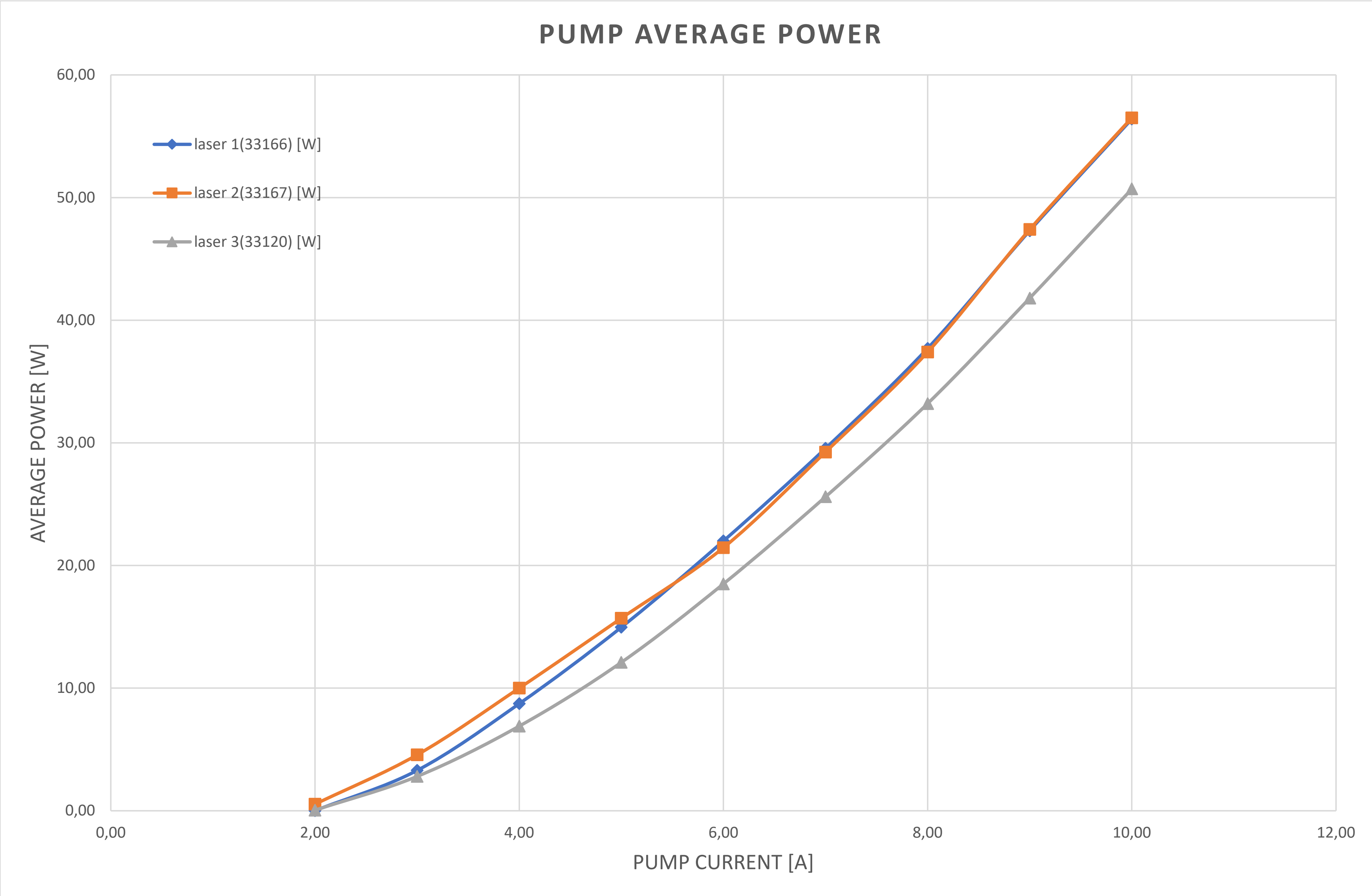

PUMP AVERAGE POWER
laser 1(33166) [W]
laser 2(33167) [W]
laser 3(33120) [W]
AVERAGE POWER [W]
PUMP CURRENT [A]
0,00
10,00
20,00
30,00
40,00
50,00
60,00
2,00
4,00
6,00
8,00
10,00
12,00

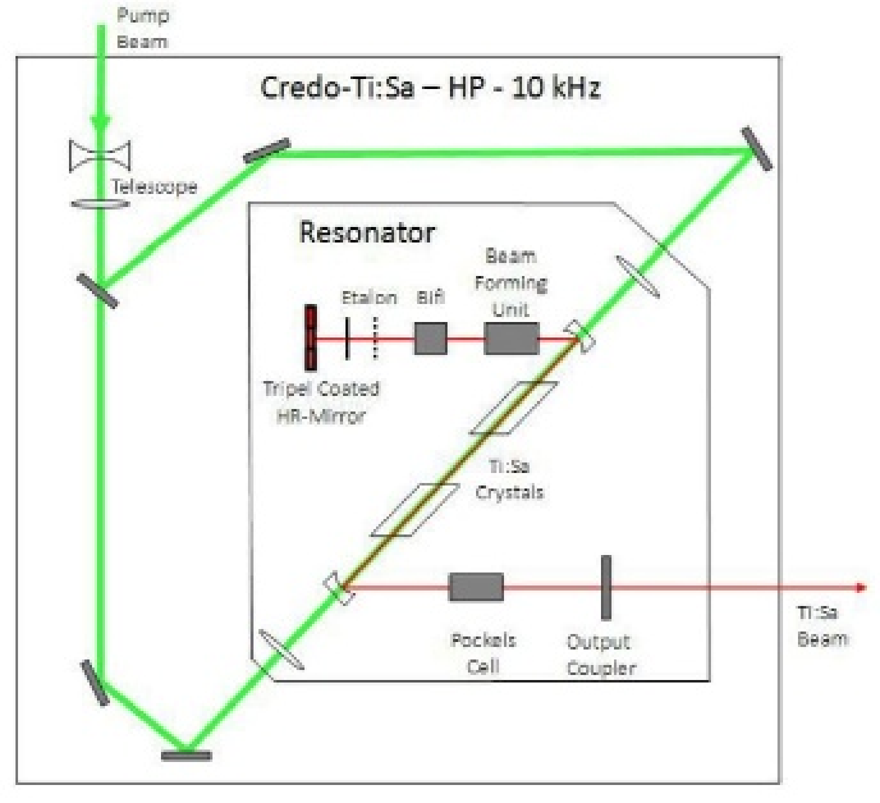
Pump
Beam
Credo-Ti:Sa – HP - 10 kHz
Telescope
Resonator
Beam
Forming
Unit
Etalon
Bifi
Tripel Coated
HR-Mirror
Ti:Sa
Crystals
Pockels
Cell
Output
Coupler
Ti:Sa
Beam

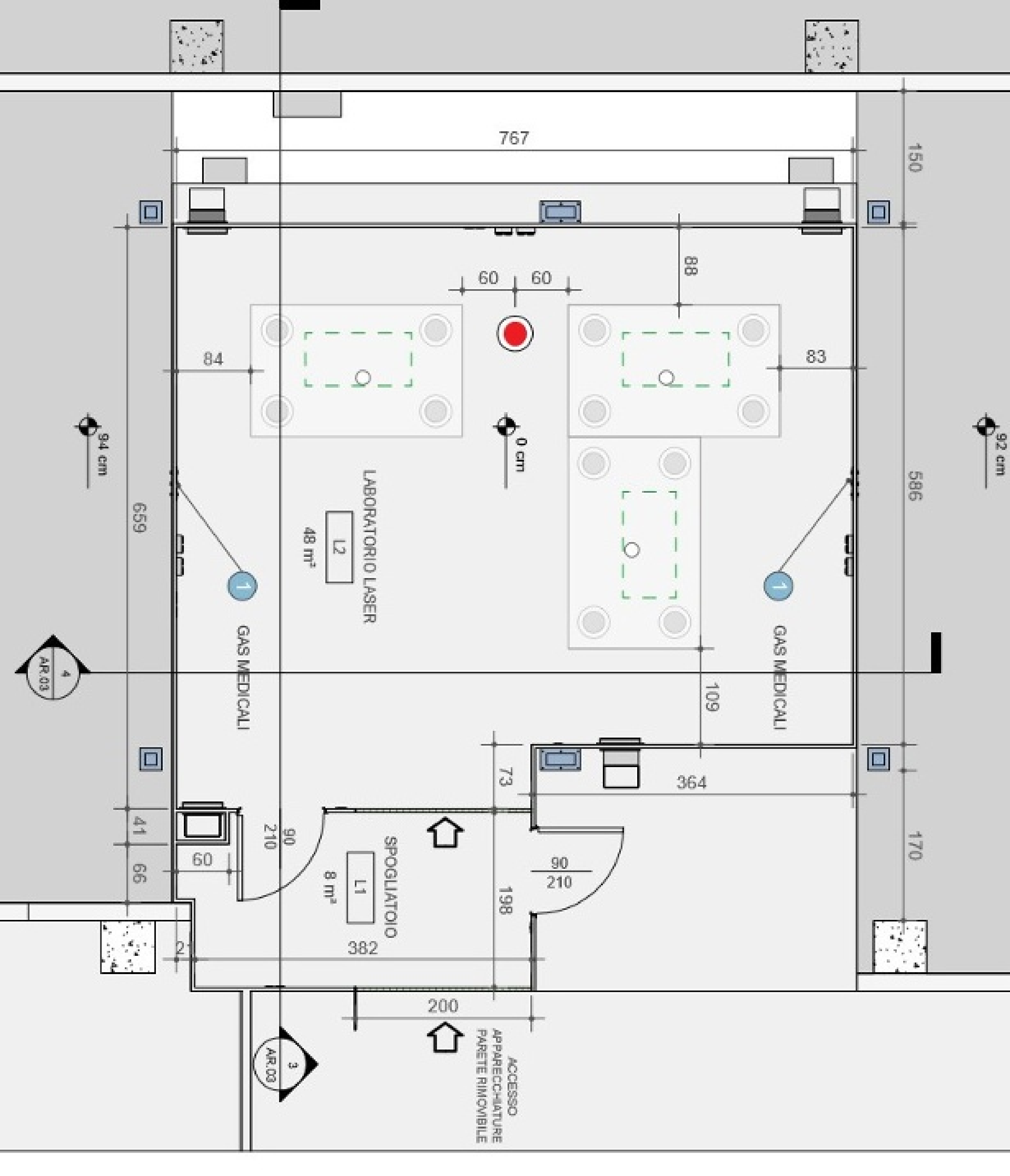

767
150
60
60
88
84
83
94 cm
0 cm
92 cm
659
586
LABORATORIO LASER
L2
48 m²
GAS MEDICALI
GAS MEDICALI
1
1
4
AR.03
109
73
364
41
66
60
90
210
SPOGLIATOIO
L1
8 m²
90
210
198
170
21
382
200
ACCESSO
APPARECCHIATURE
PARETE RIMOVIBILE
3
AR.03

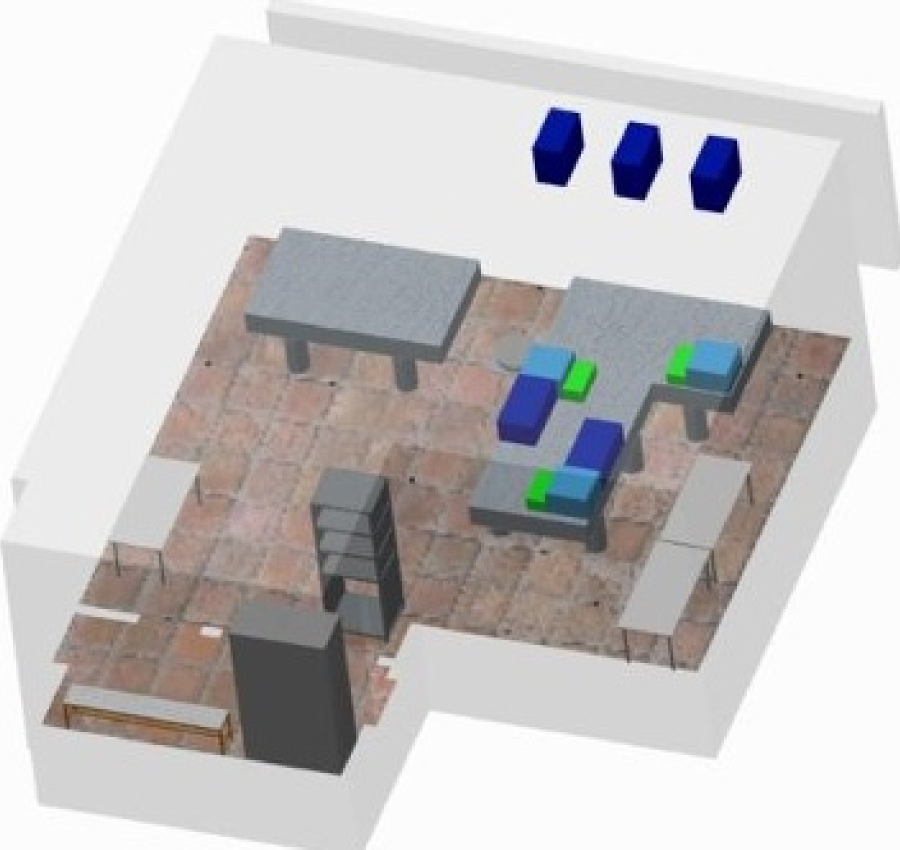

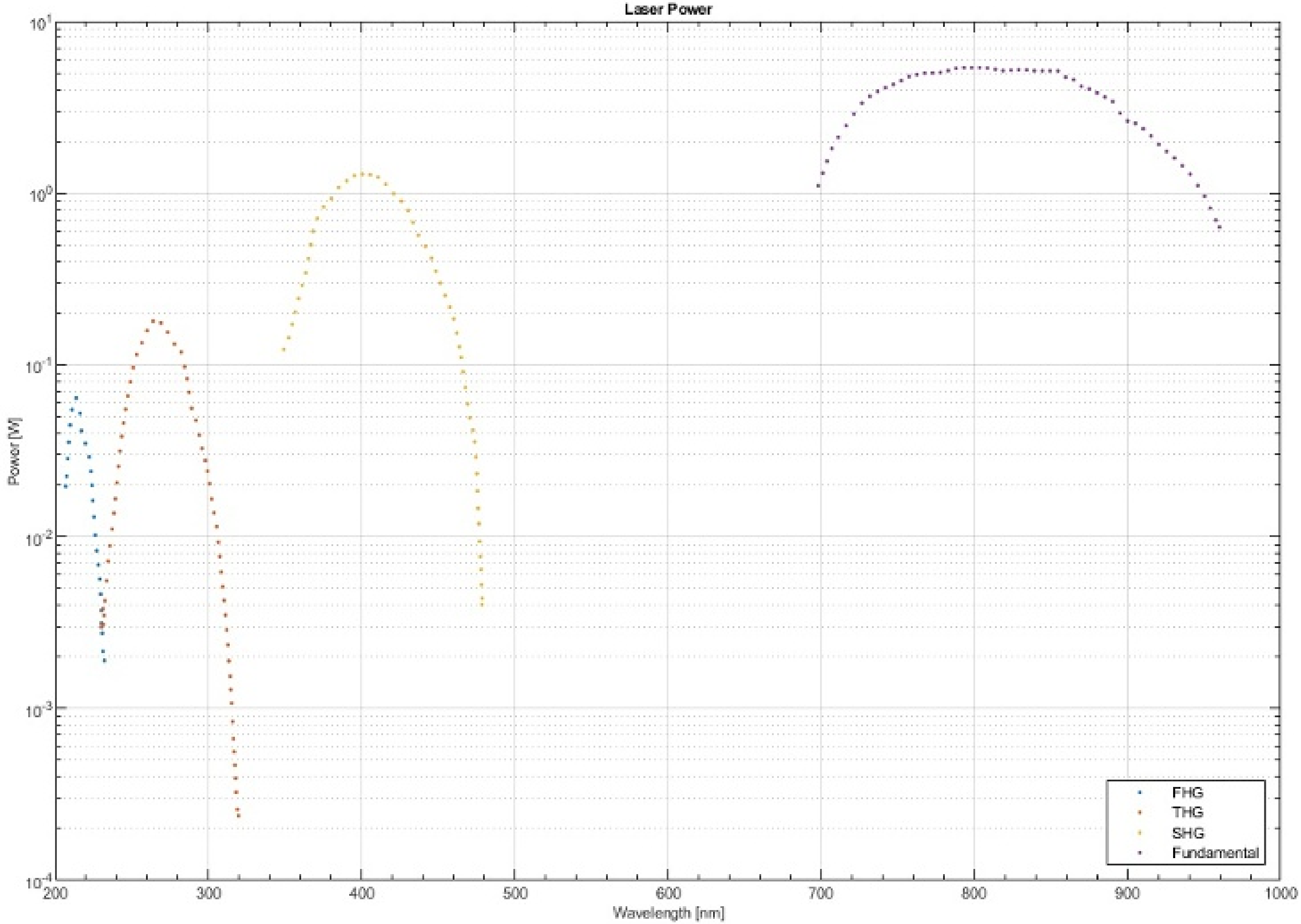

Laser Power
Power [W]
Wavelength [nm]
10^1
10^0
10^-1
10^-2
10^-3
10^-4
200
300
400
500
600
700
800
900
1000
FHG
THG
SHG
Fundamental

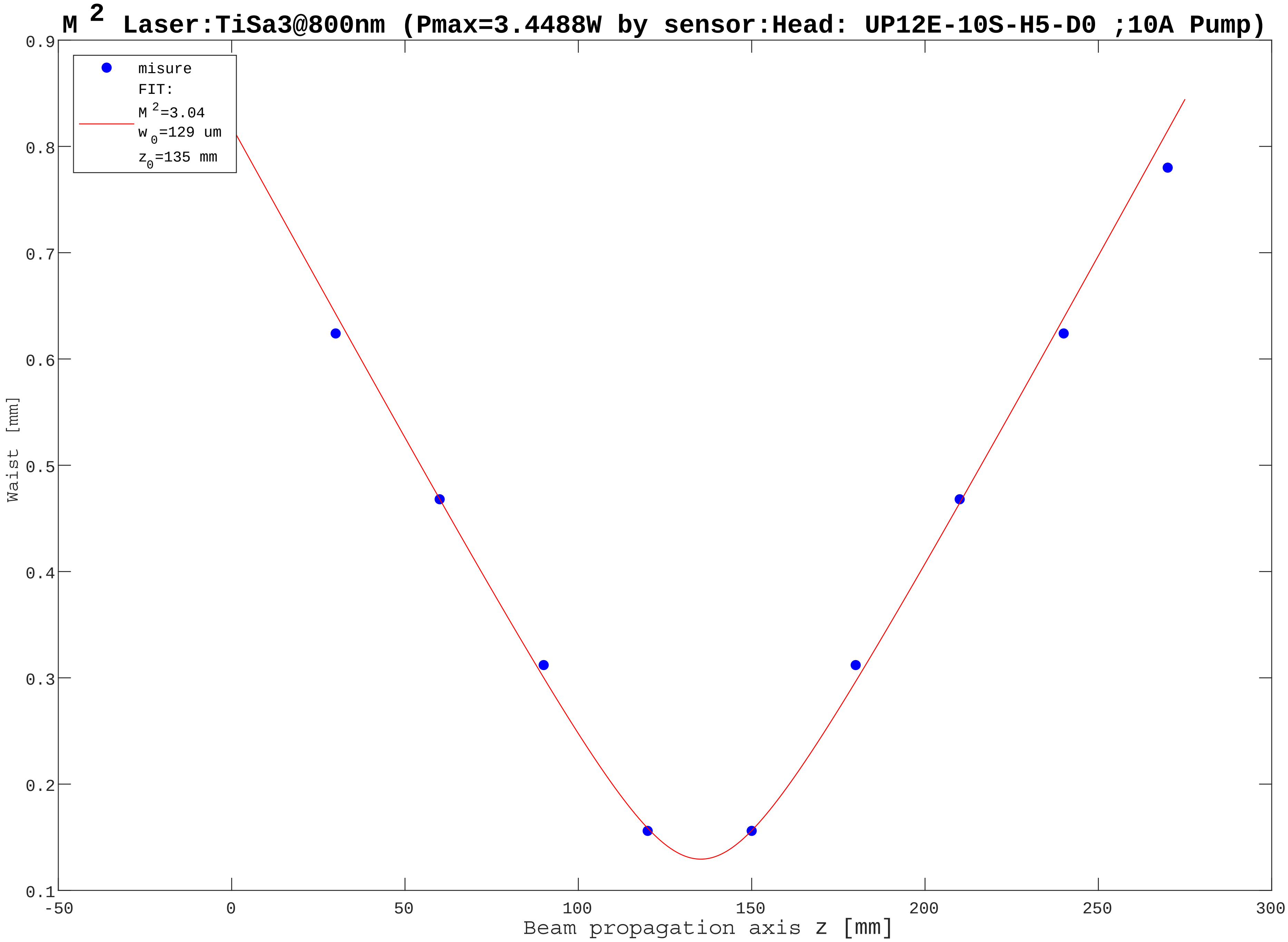
M 2 Laser:TiSa3@800nm (Pmax=3.4488W by sensor:Head: UP12E-10S-H5-D0 ;10A Pump)
misure
FIT:
M 2=3.04
w 0=129 um
z0=135 mm
Waist [mm]
Beam propagation axis z [mm]
0.9
0.8
0.7
0.6
0.5
0.4
0.3
0.2
0.1
-50
0
50
100
150
200
250
300

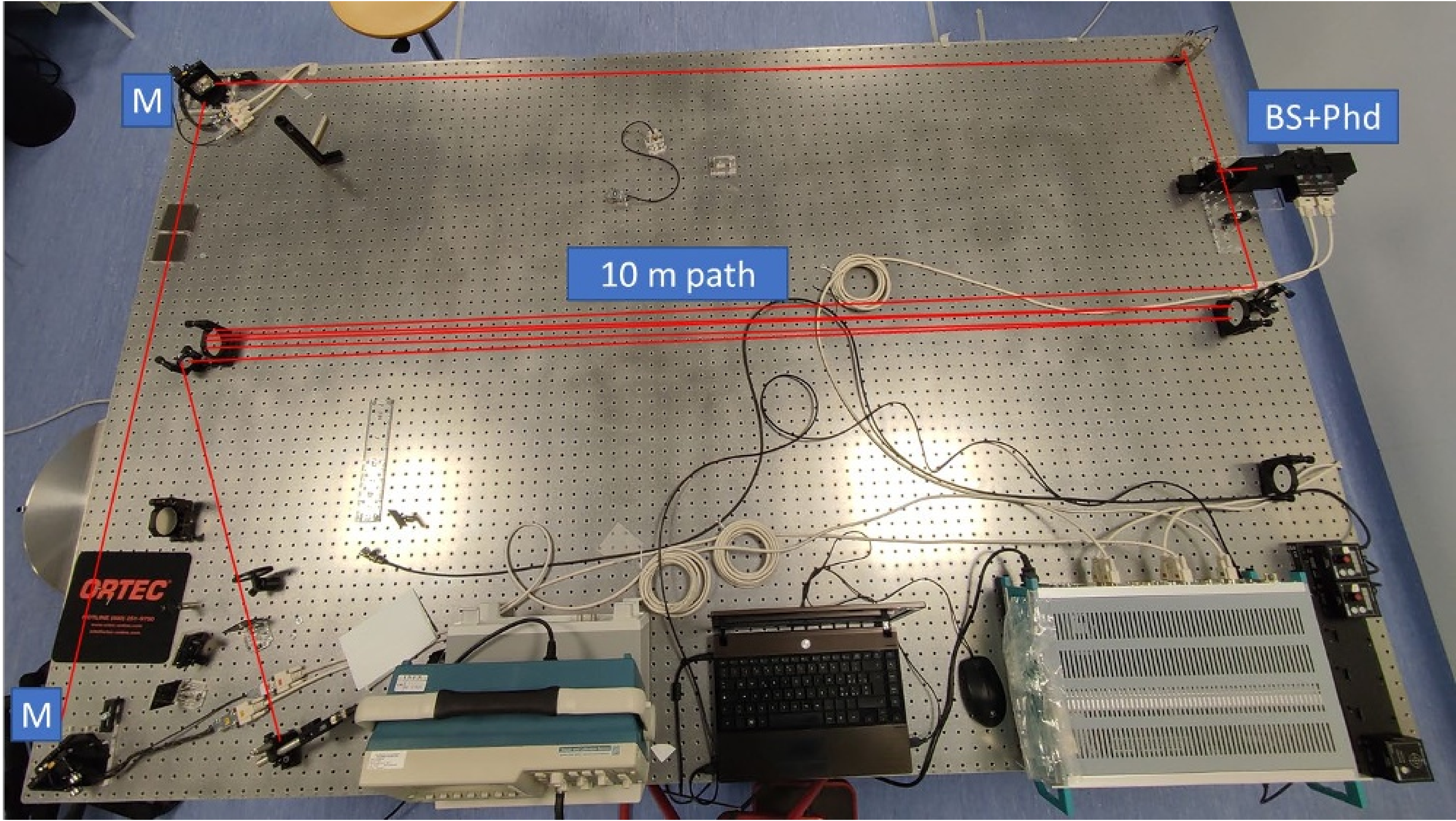
M
BS+Phd
10 m path
M
ORTEC

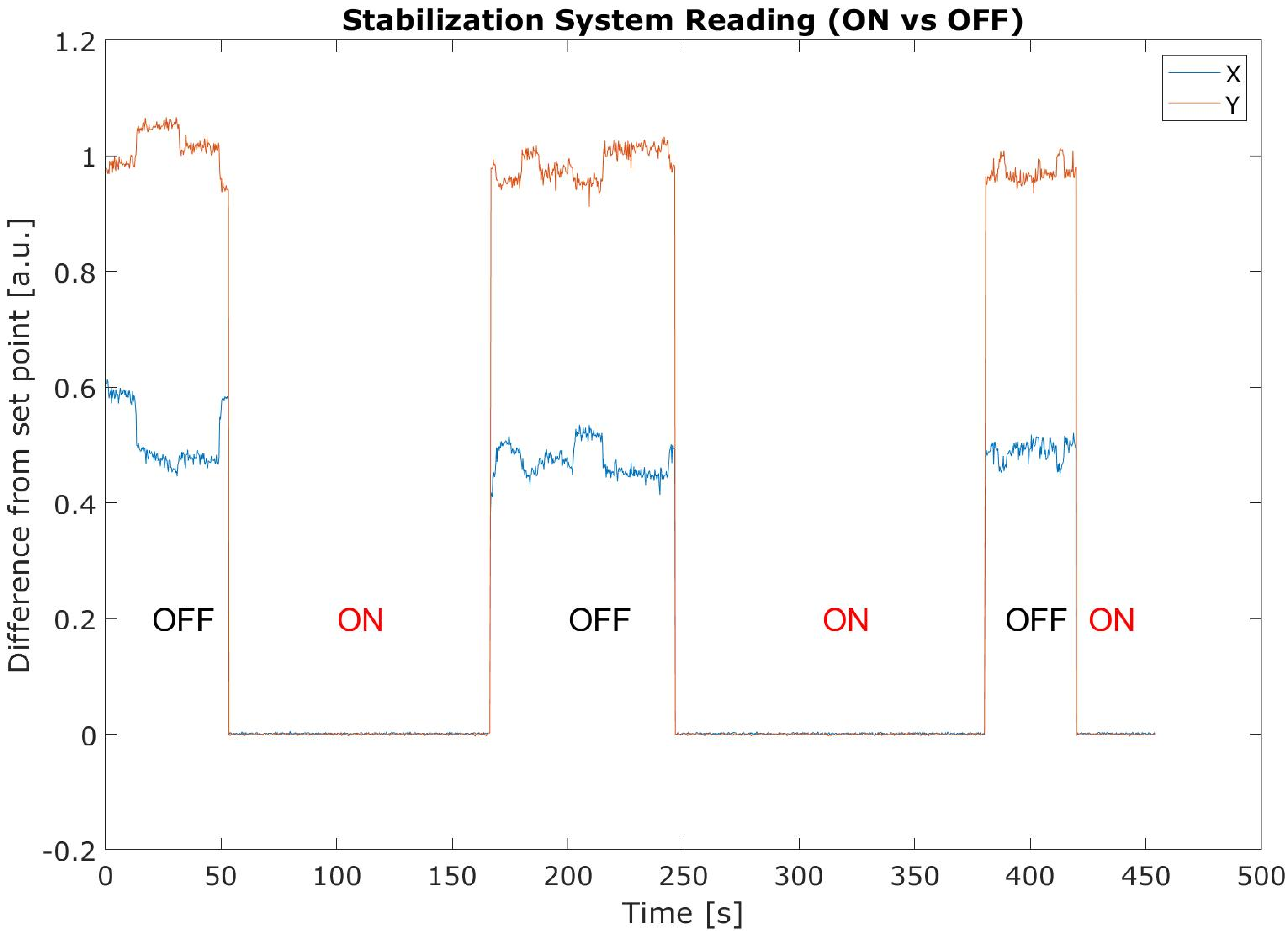
Stabilization System Reading (ON vs OFF)
Difference from set point [a.u.]
Time [s]
X
Y
OFF
ON
OFF
ON
OFF
ON
1.2
1
0.8
0.6
0.4
0.2
0
-0.2
0
50
100
150
200
250
300
350
400
450
500